Co-cultivating rice plants with *Azolla filiculoides* modifies root architecture and timing of developmental stages

Sara Cannavò[1], Chiara Paleni[2], Alma Costarelli[1], Maria Cristina Valeri[3], Martina Cerri[4], Veronica Gregis[2], Graziella Chini Zittelli[5], Petre I. Dobrev[6], Lara Reale[4], Martin M. Kater[2, †], Francesco Paolocci[3, †]*

[1] Department of Chemistry, Biology and Biotechnology, University of Perugia, Borgo XX Giugno 74, 06121 Perugia, Italy
[2] Department of Biosciences, University of Milan, Via Celoria 26, 20133 Milan, Italy
[3] Institute of Bioscience and Bioresources (IBBR), Division of Perugia, National Research Council (CNR), Via Madonna Alta, 130 06168, Perugia, Italy
[4] Department of Agricultural, Food and Environmental Sciences, University of Perugia
[5] Institute of Bioeconomy, National Research Council (CNR), Via Madonna del Piano 10, 50019 Sesto Fiorentino, Florence, Italy
[6] Institute of Experimental Botany of the Czech Academy of Sciences, Rozvojová 263, 16502 Prague 6, Czech Republic

E-mail:
casaretta93@gmail.com (Sara Cannavò)
chiara.paleni@unimi.it (Chiara Paleni)
alma.costarelli@outlook.it (Alma Costarelli)
mariacristina.valeri@ibbr.cnr.it (Maria Cristina Valeri)
cerri.martina@gmail.com (Martina Cerri)
veronica.gregis@unimi.it (Veronica Gregis)
graziella.chinizittelli@cnr.it (Graziella Chini)
dobrev@ueb.cas.cz (Petre Dobrev)
lara.reale@unipg.it (Lara Reale)
martin.kater@unimi.it (Martin M. Kater)
francesco.paolocci@ibbr.cnr.it (Francesco Paolocci)

[*] corresponding author
lara.reale@unipg.it
francesco.paolocci@ibbr.cnr.it

[†] contributed equally as last authors

Submission date: October 2, 2024
Number of tables: 1
Number of figures: 10
Word count: 7453
Supplementary tables: 12
Supplementary figures: 11

Running title:
Azolla filiculoides modifies the growth of rice plantlets

Highlight
Azolla filiculoides alters the root transcriptome and hormonal balance in both roots and leaves of co-cultivated rice plantlets, thereby interfering with the progression of their developmental programs

Abstract

Strategies for increasing the yield of rice, the staple food for more than half of the global population, are needed to keep pace with the expected worldwide population increase, and sustainably forefront the challenges posed by climate change. In Southern-East Asian countries, rice farming benefits from the use of *Azolla* spp. for nitrogen supply. In virtue of the symbiosis with the nitrogen-fixing cyanobacterium *Trichormus azollae, Azolla* spp. are ferns that release nitrogen into the environment upon decomposition of their biomass. However, if and to what extent actively growing *Azolla* plants impact on the development of co-cultivated rice plantlets remains to be understood. Here, we show that actively growing *Azolla filiculoides* plants alter the architecture of the roots and accelerates the differentiation and proliferation of leaves and tillers in co-cultivated rice plants. These changes result from an intimate cross-talk between rice and *A. filiculoides,* in which hormones and other metabolites released by the fern in the growth medium trigger an alteration in the rice root transcriptome and the hormonal profiles of both roots and leaves. Overall, the present data let us argue that co-cultivation with *A. filiculoides* might prime rice plants to better deal with both abiotic and biotic stress.

Keywords
Azolla*,* hormones, LCMS, *Oryza sativa*, nitric oxide, plant architecture, qRT-PCR, root apparatus, transcriptome, *Trichormus* (*Anabaena*) *azollae*

Abbreviations: SDGs, Sustainable Development Goals; N, nitrogen; NUE, nitrogen use efficiency; PAR, photosynthetically active radiation; N2, atmospheric nitrogen; VOCs, volatile organic compounds; RSA, root system architecture; ½MS, half-strength MS nutrients; R treatment, boxes containing sole rice plants (control); R+Af treatment, rice co-cultivated with *A. filiculoides*; DAT, Days After Transplanting; ARs, adventitious roots; LRs, lateral roots; NH_4^+, ammonium; NO_2^- nitrite ion; NO, nitric oxide; DAF-2DA , 4,5-diaminofluorescein diacetate; CTCF, corrected total cell fluorescence; NED, N-(1-naphthyl) ethylenediamine dihydrochloride; DEGs, differentially expressed genes; SPE, solid-phase extraction; IS, internal standards; ROS, reactive oxygen species; RNS, reactive nitrogen species.

Introduction

Rice (*Oryza sativa*) is a staple food crop for more than half of the global population, which is expected to reach almost 10 billion in 2050 (UN 2022). As global demand for major crops will roughly double by 2050, agricultural production may need to be increased by 70%–110% (FAO, 2009a; Tilman *et al.*, 2011). Unfortunately, the increase in the size of the human population is paralleled neither by the yield increase of rice nor by any other agricultural products (Godfray *et al.*, 2010; Alexandratos and Bruinsma, 2012; FAO, 2009a, b, 2022a, 2022b). The stagnation of crop yields has several underlying reasons, including loss of genetic diversity in today's crop species (Day, 1973; Gaillard *et al*., 2018; Mueller *et al*., 2012). Moreover, the increasing temperature, rising sea levels, and alterations in rainfall patterns and distribution caused by global climate change could lead to substantial modifications in land and water resources for rice production as well as in the productivity of rice crops grown in different parts of the world (Nguyen, 2002). Therefore, the ongoing climate change poses a further obstacle to assuring food security and achieving the most significant Sustainable Development Goals (SDGs) set by the UN (https://sdgs.un.org/goals).

Rice yield decline has also been related to decreased physiological nitrogen (N) use efficiency (NUE). This occurs in intensive rice cultivation systems under tropical conditions and when rice is grown under temperate conditions, where N is supplied as urea or green manure (Lhada *et al*., 2000; Casanova *et al*., 2002). Yet, in Southern-East Asian countries, the aquatic ferns belonging to the *Azolla* genus have been traditionally used in rice farming as N supplier crops either as a mono-crop, when they are incorporated into the soil before rice transplanting, or as intercrop, when grown as a dual crop along with rice (Fogg *et al*., 1973; Lumpkin and Plucknett, 1980; Shi and Hall, 1988; Watanabe, 1982; Watanabe and Liu, 1992; Yang *et al.*, 2018). Depending on the cropping system, the presence of the fern can increase rice productivity by 30-50% (Marzouk *et al*., 2023), and this increase has been mainly related to increased NUE. *Azolla* spp. are in fact perennial, monoecious floating freshwater ferns that live in a permanent mutualistic symbiosis with the nitrogen-fixing cyanobacterium-*Trichormus azollae* and other species-specific endophytic prokaryotic strains. The association *Azolla-T. azollae* is capable of fixing N_2 at a rate that rivals that of *Rhizobium*-legume symbiosis (Lumpkin and Plucknett, 1980). However, nitrifying bacteria and other plants do not benefit from this low-cost source of N_2, as the cyanobacteria keep 60% whereas the remaining 40% of the fixed nitrogen is immediately translocated to Azolla (Peters and Meeks, 1989). Only a negligible amount (3-4%) of ammonium (NH_4^+) of the total nitrogen fixed by *T. azollae* is released into the water. The remaining 96-97% of the fixed N_2 is therefore unavailable to other plants until the Azolla biomass is mineralized. This suggests that the Azolla nitrogen-rich biomass is released into the soil only following plant death and decomposition (Mahanty et al., 2017).

Additionally, Azolla considerably modifies the physico-chemical and biological properties of water, controls weed, algae, insects and pest proliferation, thereby reducing resource losses and management costs in rice farming (Herath, 2023). Thanks to these features, Azolla has been recently reconsidered as an eco-friendly and innovative solution to replace or integrate chemical nitrogen fertilizers and pesticides to improve rice yield sustainability even under suboptimal conditions (Yao *et al*., 2018; Khumairoh *et al*., 2018). Although many experiments have demonstrated the increase in the root and shoot growth and, ultimately, weight of grains in rice as a consequence of co-cultivation with Azolla (Bhuvaneshwari and Singh, 2015), the benefit of Azolla on rice varies greatly also according to the climate, the species of Azolla used, and many other factors (Wagner, 1977, Tung and Shen 1985). Studies have documented the competence of both *Azolla* spp. and the endosymbionts hosted in their fronds to synthetise and release metabolites such as siderophores, phytohormones, and volatile organic compounds (VOCs) that might interfere with the developmental patterns of the nearby plants (Vlek *et al*., 2002; Banach *et al*., 2019; Valette *et al.*, 2020; Brilli *et al*. 2022). However, the mechanisms underlying the various growth-promoting effects of Azolla on rice are still partially

unknown, especially those that may occur during co-cultivation. For instance, the answers to the question of whether Azolla can improve NUE in rice by modifying its root system architecture (RSA) and if it does so not only because it provides N but also via the secretion of growth-promoting substances remain elusive.

The present study focuses on the hypothesis that Azolla is more than a N supplier for rice. In our experimental setup, we cultivated rice plants in the presence of actively growing *Azolla filiculoides* plants to prevent an extra nitrogen supply to rice compared to the control condition (rice plants alone) and gain insights into the morphogenetic effects that *A. filiculoides* has on young rice plants. To reach this goal, the morphological monitoring of rice root apparatus and aerial organs' development was coupled with rice root transcriptomics and hormonal profiles of rice roots, leaves, and growth media. Our results demonstrate that *A. filiculoides* interferes with the patterns and timing of rice root and aerial organs' development by modulating rice root transcriptional profiles and the hormonal balance in both rice roots and leaves.

Materials and Methods

Plant material and growth conditions

A. filiculoides, collected from a small pond of the botanical garden of the University of Perugia–Italy and characterized as reported in Costarelli *et al*. (2021), was grown in a climatic chamber under a 14 h light photoperiod at an irradiance of 220 µmol m^{-2} s^{-1} (photosynthetically active radiation - PAR) and a light/dark temperature of 25/19°C. The solution employed for *A. filiculoides* stock maintenance was the Watanabe's growth solution (Watanabe *et al.*, 1992), which was completely replaced every 7 days and refilled when necessary. Once a week, *A. filiculoides* stock cultures were split to avoid overcrowding and gently disentangled to favour growth. After removing the hull with tweezers, the seeds of rice *Oryza sativa* L. var. Kitaake were surface sterilized with ethanol for 30'', followed by 30' in 30 mL of commercial bleach and 2 µL of Tween20 in falcon tubes under continuous shaking. Afterward, 8-10 washes with sterile water were performed under a laminar flow hood. Seeds were left in imbibition in the dark o/n. The seeds were sowed in Petri dishes containing half-strength MS nutrients (½MS) (Murashige and Skoog, 1962) for 2 days in the dark at 30°C for germination, and successively in Magenta boxes for 10 days for seedlings growth. Four 13-day-old seedlings per replicate were then transplanted into specifically designed plex hydroponic boxes (230x230x150 mm) harbouring 4 pivots sticking out of the base and containing ca. 5 L of Yoshida's nutritive solution (Gregorio *et al*., 1997). Each pivot could hold a hydroponics net pot that, once filled with expanded clay taken in place by a piece of non-woven tissue, supported rice growth for the entire duration of the experiment. Boxes containing sole rice plants (control, hereinafter referred to as R treatment) or rice co-cultivated with *A. filiculoides* (hereinafter referred to as R+Af treatment) were kept in a growth chamber under the conditions described above for *A. filiculoides* maintenance. The surface of the boxes without Azolla were covered and the walls of all the boxes wrapped with aluminium foil to prevent the development of algae. The growth solution was completely replaced every 2 weeks and refilled when necessary. No water-aeration system was applied and, when necessary, dying *A. filiculoides* plants substituted with fresh ones to ensure the same level of Azolla coverage. Unless differently specified, at least three boxes per treatment with four rice plants each were employed as replicates for each experiment and the entire experimental set up was run three times.

Morphological analysis of rice plantlets

Number of leaves and tillers and the height of rice plants grown under R+Af and R treatments were scored every week for 63 days from the start of the hydroponics cultivation, herein after referred to as Days After Transplanting (DAT). Root architecture and fresh/dry plant weight were monitored at

15, 30, and 60 DAT by harvesting 1 plant for each replicate. The harvested plants were dipped in water to remove the adhering clay particles and other macroscopic contaminants and then carefully dried. The length of adventitious (ARs) and lateral (LRs) roots and that of shoots were measured using a ruler. Roots were then detached from the stems to measure the fresh weight of below and above water surface organs. The number of ARs and tillers were counted in all plants, whereas the number of ARs with and without LRs were counted in a subset of 3 plants per treatment. Portions of ARs, collected at 150 mm from the base of the stem, were observed at the epifluorescence light microscope (excitation 495 nm; emission 515 nm; long-pass filter of 515 nm) to determine the frequency of LRs (expressed as number/mm). The dry weight of root and leaves was measured by treating a portion of these organs in the oven at 80°C until a constant weight was reached.

Determination of inorganic nitrogen content in culture media

The concentration of different forms of inorganic nitrogen in the media from R and R+Af treatments was evaluated at 10, 20 and 30 DAT. NH_4^+ concentration was assessed by the spectrophotometric absorbance at 690 nm of a derivative of indophenol formed by reaction of sodium salicylate and chlorine ammonia in an alkaline environment as reported in Jeong and colleagues (2013). The absorbance at 420 nm of the products resulting from the reaction between nitrates and sodium salicylate in acid solution for sulfuric acid was employed to assess the levels of $N0_3^-$ (Monteiro *et al*., 2003). NO^{2-} was determined following Monteiro *et al*. (2003): at pH 2.0-2.5 the sulfanilamide (I) is diazotized by nitrous acid and the resulting diazo compound is coupled with N-(1-naphthyl)-ethylenediamine (II) to form an azocompound that absorb at 543 nm (Monteiro *et al*., 2003; Jeong *et al*., 2013).

Nitric oxide quantification in rice roots

Nitric Oxide (NO) was analysed in the AR apex cells of rice grown under R+Af and R treatments at 15 and 30 DAT. NO yellow–green fluorescence was detected by epifluorescence light microscopy (excitation 495 nm; emission 515 nm; long-pass filter of 515 nm) after incubation of a root portion in the dark in 10 μM 4,5-diaminofluorescein diacetate (DAF-2DA) for 3 h at RT (Kojima *et al.*, 1998). DAF-2DA permeates through the cell membrane and was hydrolysed to DAF-2, which was retained in the cell owing to its relatively poor permeability. DAF-2 reacts with NO to form fluorescent DAF-2 T. NO content in the roots of rice grown with and without *A. filiculoides* were computed using ImageJ v. 1.4 and the corrected total cell fluorescence (CTCF) was calculated as:

$$\text{CTCF} = \text{Integrated Density} - (\text{Area of selected cell} \times \text{Mean fluorescence of background readings})$$

NO contents were also evaluated via the colorimetric Griess assay according to manufacturer instructions (Sigma-Aldrich). The oxidation product of NO, nitrite, reacts with sulfanilamide and N-(1-naphthyl) ethylenediamine dihydrochloride (NED) to yield a pink stable azo product. The conversion of spectrophotometric absorbance values recorded at 548 nm to nitrite concentration, and hence indirectly NO, was possible using the linear regression of the calibration curve (Vishwakarma *et al.*, 2019). The calibration curve was done according to the manufacturer instructions and NO content was calculated by comparison with a standard curve of $NaNO_2$ as described in Zhou *et al.* (2005).

Rice root transcriptomics analysis

To collect samples for untargeted RNA analysis, rice plants from both treatments were rinsed with distilled water and the distal portions, up to 1 cm from the apices, of rice roots were cut with a sterile blade and immediately frozen in liquid nitrogen. If necessary, samples from different plants were pooled. RNA from the roots of three biological replicates per treatment at 15 DAT was isolated with Qiagen RNeasy Plant Mini Kit and treated with Qiagen Rnase-Free Dnase Set. Stranded mRNA

226 libraries were prepared by Novogene with poly-T oligo-attached magnetic beads, followed by random
227 hexamer priming and second strand cDNA synthesis with dUTP. The libraries were sequenced in
228 paired-end 150bp mode on Illumina platform. To remove adapters, incomplete reads and low-quality
229 reads, raw reads were filtered and quality-trimmed with Fastq-mcf (Aronesty, 2011) with options -l
230 50 -q 30 and quality of read sets was assessed with FastQC (Andrews, 2021) and MultiQC (Ewels *et*
231 *al.*, 2016). Reads were mapped on Oryza sativa cv. Nipponbare Os-Nipponbare-Reference-IRGSP-
232 1.0 with annotation version 2022-03-11 (downloaded from the RAP-DB database, available at
233 rapdb.dna.affrc.go.jp/download/irgsp1.html) (Kawahara *et al.*, 2013; Sakai *et al.*, 2013). For
234 mapping, reads alignment and transcript quantification were performed with Rsem v1.3.3 (Li and
235 Dewey, 2011). Count tables were imported in R v4.0.2 with package TxImport v1.16.1 (Soneson et
236 *al.*, 2015) and differential gene expression analysis between growth conditions was performed with
237 DeSeq2 v1.28.1 (Love, Huber and Anders, 2014). Finally, the list of differentially expressed (DE)
238 genes with criteria |logFC|> 0 and padj ≤ 0.05 (unless specified otherwise) was selected to run
239 functional enrichment analysis on ShinyGO v0.76 (Ge *et al.*, 2020), using the set of terms from Gene
240 Ontology (Biological project, Molecular Function and Cellular Component) and KEGG, and using
241 the list of all genes with detectable expression as background. ShinyGO was also used to investigate
242 differentially expressed genes (DEGs) and produce a network summarizing enriched pathways.
243 Pathways were linked when they shared at least 20% of genes. The resulting network was visualized
244 on CytoScape v3.9.1 (Shannon *et al.*, 2003).
245

246 *Validation of RNA-seq data by qRT-PCR*

247 To validate the dataset obtained by RNA-seq analysis, the expression of a subset of DEGs was
248 monitored by quantitative reverse transcriptase PCR (qRT-PCR) analysis. In Table S1 are given the
249 12 target genes and the 4 housekeeping genes amplified along with their primer pairs. Total root RNA
250 was isolated from an independent experimental set of rice samples compared to those employed for
251 RNA-seq analysis. Root samples, collected as reported in the previous paragraph, were taken at 0, 5,
252 9, 12 and 15 DAT. One and half µg of RNA isolated as reported above was reverse-transcribed in the
253 presence of Maxima H Minus Reverse Transcriptase (Thermo Fisher Scientific, Milan, Italy) and 100
254 pmol of random hexamers (Euroclone, Milan, Italy), in a final volume of 20 µL. An aliquot of 2 µL
255 of 1:10 diluted cDNA was used in the PCR reaction, which was carried out using the BlasTaq 2X
256 qPCR Mater Mix (ABM, Richmond, Canada) in an Light Cycler 86 apparatus (Roche) using the
257 following cycling parameters: an initial step at 95°C for 60'', 30 cycles of a step at 95°C for 10'' and
258 a step at 60°C for 30'', followed by a high resolution melting curve performed as: 95°C for 60'',
259 40°C for 60''; 65°C for 1'' and 97°C for 1'', prior to the cooling step at 37°C for 60''. For each gene,
260 time point and biological samples four technical replicates were amplified. For each primer pair, the
261 efficiency of PCR was tested as reported previously (Escaray *et al*., 2014). The $2^{-\Delta Ct}$ gene expression
262 quantification method was applied to compare the relative expression levels among the target genes
263 (Bizzarri et al. 2020). Here, the $2^{-\Delta Ct}$ method was based on the differences between the relative
264 expression levels of the target genes and the geometric mean of the 4 housekeeping genes described
265 in de Castro Dos Santos *et al*. (2018).
266

267 *LCMS analysis of phytohormones in rice roots, leaves and growth media.*

268 Extraction and purification of phytohormones from plant material (i.e., rice roots and leaves) and
269 growing media at 0 and 15 DAT were performed by solid-phase extraction (SPE) followed by LCMS-
270 QQQ according to a previously published protocol with minor modifications (Prerostova *et al.*, 2021).
271 Root sampling was performed as reported for RNA-seq and qRT-PCR analyses. For leaf sampling,
272 the median part of the most expanded leaves was collected. For the media, 1 ml aliquots were
273 collected for each box and then lyophilized. Tissue disruption (30mg) was performed in 100 µL
274 extraction solvent (1M HCOOH) using a benchtop homogenizer FastPrep-24 (MP Biomedicals, CA,

275 USA) in an extraction solvent and about 0.05 g of 1.5 mm zirconiumoxide balls. This step was not
276 performed on media samples, which were resuspended in 100 µL of extraction solvent. Ten µL of the
277 internal standards (IS) were added to the samples, thoroughly mixed and centrifuged at 4°C and
278 30,000*g*. The resultant supernatants were gently collected and applied to the SPE plate. The following
279 isotope-labelled mixture was added to each sample: $^{13}C_6$-IAA (Cambridge Isotope Laboratories,
280 Tewksbury, MA, USA); $^{2}H_4$-SA (Sigma-Aldrich, St. Louis, MO, USA); $^{2}H_3$-PA, $^{2}H_3$-DPA (NRC-
281 PBI); $^{2}H_6$-ABA, $^{2}H_5$-JA, $^{2}H_5$-tZ, $^{2}H_5$-tZR, $^{2}H_5$-tZRMP, $^{2}H_5$-tZ7G, $^{2}H_5$-tZ9G, $^{2}H_5$-tZOG, $^{2}H_5$-tZROG,
282 $^{15}N_4$-cZ, $^{2}H_3$-DZ, $^{2}H_3$-DZR, $^{2}H_3$-DZ9G, $^{2}H_3$-DZRMP, $^{2}H_7$-DZOG, $^{2}H_6$-iP, $^{2}H_6$-iPR, $^{2}H_6$-iP7G, $^{2}H_6$-
283 iP9G, $^{2}H_6$-iPRMP, $^{2}H_2$-GA_1, $^{2}H_2$-GA_4, $^{2}H_2$-GA_8, ^{2}H2-GA_{12}, $^{2}H_2$-GA_{19}, ^{2}H2-GA_{34}, ($^{2}H_5$)($^{15}N_1$)-IAA-
284 Asp, ($^{2}H_5$)($^{15}N_1$)-IAA-Glu (Olchemim, Olomouc, Czech Republic), ($^{2}H_5$)($^{15}N_1$)-IAM, $^{2}H_5$-IAA-
285 GE+Am, $^{2}H_4$-OxIAA, $^{2}H_4$-OxIAA-GE+Am and $^{2}H_3$-epi-Br.
286 The 96-well SPE plates (Oasis HLB 10 mg sorbent per well; Waters, Milford, MA, USA) were
287 activated by sequentially applying 100 µL of acetonitrile, water and extraction solvent for 3 minutes.
288 Pressure was applied to pass the samples through the extraction columns using a Pressure+96 positive
289 pressure manifold (Biotage, Uppsala, Sweden). Pellets were re-extracted with an additional 100 µL
290 of extraction solvent, centrifuged and applied again to the column plates. The wells were then washed
291 3 times with 100 µL of water. The phytohormones were eluted with 2 x 50 µL elution solvent (50%
292 ACN in water). The eluate was collected in a collection plate, sealed with the 96-well silicone cap
293 and stored at -20°C until LCMS analysis. Phytohormones were separated on Kinetex EVO C18
294 column (2.6 µm, 150 x 2.1 mm, Phenomenex, Torrance, CA, USA). Mobile phases consisted of A—
295 5mM ammonium acetate and 2 µM medronic acid in water and B—95:5 acetonitrile:water (*v/v*). The
296 following gradient was applied: 5% B in 0 min, 5–7% B (0.1–5 min), 10–35% B (5.1–12 min) and
297 35–100% B (12–13 min), followed by a 1 min hold at 100% B (13–14 min) and return to 5% B.
298 Hormone analysis was performed using an LCMS system consisting of a UHPLC 1290 Infinity II
299 (Agilent, Santa Clara, CA, USA) coupled to a 6495 Triple Quadrupole Mass Spectrometer (Agilent,
300 Santa Clara, CA, USA) operating in MRM mode, with quantification by the isotope dilution method.
301 Data acquisition and processing were performed using Mass Hunter software B.08 (Agilent, Santa
302 Clara, CA, USA). The amounts of the quantified compounds were expressed as pmol/gFW and
303 pmol/mL. Outliers were identified by statistical test (i.e., interquartile range IQR) and excluded for
304 subsequent analysis in MetaboAnalyst (version 5.0) (Pang et *al.*, 2021).
305

306 T. azollae *growing conditions and phytohormone analysis of the medium*

307 The cyanobacterium *T. azollae* used in this study was obtained from the Culture Collection belonging
308 to the Institute of BioEconomy (IBE), National Research Council of Italy (CNR; Sesto Fiorentino,
309 Firenze, Italy). The cyanobacterium was cultivated in laboratory in batch mode using vertical glass
310 column reactors (5 cm light path, 600 ml working volume) and BG110 (nitrogen-free) as culture
311 medium (Rippka *et al.*, 1979). Continuous illumination of 40 µmol m^{-2} s^{-1} (PAR) was provided by
312 means of cool white lamps (Dulux L, 55W/840, Osram), and a culture temperature of 22 ± 2°C was
313 maintained by thermostat-cultivation room. Cultures were bubbled with a sterile air/CO_2 mixture
314 (98/2, v/v) to ensure continuous mixing, remove dissolved oxygen, and maintain pH within the
315 desired range (7.5–8.0). The cultures were diluted once a week by repeating the same growth cycle
316 three times (i.e., 200 mL of culture was removed and processed, and the same volume of fresh culture
317 medium added). For phytohormone analysis of the *T. azollae* medium, samples were taken in sterile
318 conditions, centrifuged at 4,000 *g* for 25', the supernatant filtered (pore size 0.45 µm), aliquoted into
319 vials and stored at -20°C until analysis.
320

321 *Statistical analysis*

322 Rice plants were grown with and without *A. filiculoides* and experiments were repeated thrice. For
323 each treatment, 12 to 16 plants were independently computed unless specified otherwise. To

determine significant differences between treatments, data were tested for homogeneity of variance (F-test or Levene's test) and normality distribution (Shapiro-Wilk's test). If the assumptions of these tests were not violated, data were analyzed via unpaired two-sample t-test or via one-way analysis of variance (ANOVA) and post hoc comparison (Tukey's HSD), according to the number of treatments. If the assumptions of the homogeneity of variance or normality distribution tests were violated, data were analyzed via the Wilcoxon rank sum test. Statistical analyses were carried out in R studio (version 3.5.3) (R Core Team, 2016) or in MetaboAnalyst (version 5.0). The level of significance was set to $P < 0.05$ or to FDR cut-off < 0.05 and treatment mean values ± S.E. were plotted unless differently specified. To analyze targeted-harmonics data, multivariate statistics allowed for the computation of sPLSD and respective Loadings plot after data normalization by median and Pareto scaling (i.e., mean-centered and divided by the square root of the standard deviation of each variable). Statistical analysis was performed both at the same time point between treatments and over time within the same treatment.

RESULTS

The co-cultivation with A. filiculoides *changed rice root architecture and induced a NO boost in the rice adventitious roots*

To investigate the effects of *A. filiculoides* on rice RSA, the number and length of ARs, LRs, and the root weight in the R+Af and R treatments were measured at 15, 30, and 60 DAT. A significant increase in the number of ARs was seen in the presence of *A. filiculoides* (Fig. 1A) at 30 DAT. At the same time point, the length of the ARs in the R+Af treatment was shorter (Fig 1B), whereas at 60 DAT, for this trait, an opposite pattern was observed (Fig. 1B). The number of ARs provided with and without LRs, the length of LRs and the number of LR/mm were also evaluated in R and R+Af treatments at 15 and 30 DAT. Conversely, the monitoring of these parameters at 60 DAT was prevented by the extensive root mats adhering to the clay and the pot in all plants. At 15 DAT, the number of ARs provided with and without LRs was not significantly different between the treatments (Fig. 1C). Rather, at 30 DAT the number of ARs provided with LRs was significantly higher in the R+Af compared to the R treatments (Fig. 1D). Differently, the number of thick, unbranched ARs and the ratio of the number of ARs having LRs divided by that without LR (AR +LR/-LR) were not significantly affected. The length (μm) and the number/mm of rice LRs were neither significantly different at 15 nor 30 DAT (data not shown). At 15, 30 and 60 DAT no significant differences between the two treatments were observed for the root weight. However, in the presence of *A. filiculoides* the root biomass increased of 32% and 48% at 30 and 60 DAT, respectively. It is worth noticing that the P value of the comparison between treatments at 60 DAT was $P = 0.06$ (Fig. S1).
To gain a preliminary insight into the physiological events underlying the observed effects of *A. filiculoides* on rice RSA, the relative content of NO in the ARs from R and R+Af treatments was evaluated at 15 and 30 DAT by fluorescence analysis, and the Griess assay. Both analyses showed a significant increase in NO content in the ARs of rice grown in the presence of *A. filiculoides* at 15 DAT (Fig. 2; Fig S2).

A. filiculoides *improved vegetative growth of rice plants and modified carbon allocation over time*

The fern affected the growth of rice above-ground organs over time (Fig. 3). A significant increase in the number of leaves (Fig. 3A), plant height (Fig. 3B), and number of tillers (Fig. 3C) in the R+Af vs R treatment started to appear at 28, 14 and 28 DAT, respectively. However, the significance in the number of tillers was lost after 60 DAT. The biomass of rice grown under the two treatments was

372 measured at 15, 30 and 60 DAT (Fig. S3). The aerial part and total rice weights tended to be slightly
373 lower in the R+Af compared to the R treatment at 15 DAT, whereas at 30 DAT they significantly
374 increased at 62.5% and 54%, respectively, and total plant fresh weight became higher in the R+Af
375 than in R treatment (Fig. S3B). The increase in rice total biomass in the R+Af treatment at 30 DAT
376 primarily resulted from that of the aerial part rather than from the roots (Fig. S1). At 60 DAT, the
377 above-ground part and total rice weight again tended to be higher in the R+Af compared to the R
378 treatment (P = 0.057; 58 and 74% increase, respectively). To assess whether *A. filiculoides*
379 significantly affected rice carbon allocation over time, the root/shoot ratio of the fresh weights (FWs)
380 at 15, 30, and 60 DAT were computed (Fig. 3D). A statistically significant decline was observed in
381 the R+Af treatment vs R treatment at 30 DAT. At 60 DAT, the root-to-shoot ratio showed an opposite
382 trend, as it tended to be higher in the R+Af treatment. Thus, co-cultivation with *A. filiculoides* affected
383 carbon allocation in rice at 30 DAT, that is when rice in the R+Af treatment allocated significantly
384 more carbon towards the aerial part compared to the root system in the R+Af treatment.
385

386 *The inorganic nitrogen content did not increase in the media of co-cultivated rice*

387 To investigate whether the changes in morphology and developmental timing of rice organs upon co-
388 cultivation with *A. filiculoides* were related to the increase of inorganic N in the growth media, the
389 levels of inorganic N forms were assessed at 3 time points, namely 10, 20 and 30 DAT. At any time
390 point, the levels of inorganic N increased in the media where *A. filiculoides* was present (Table S2).
391 Rather, some inorganic forms decreased in the media with *A.filiculoides,* although only at the first
392 time points.
393

394 A. filiculoides *altered rice root transcriptome at 15 DAT*

395 Morphological changes triggered by *A. filiculoides* in rice plants occurred at 30 DAT for the roots
396 and a few days earlier for the aerial parts. By reasoning that these changes resulted from signals
397 exchanged at root levels between the fern and rice plants since the early stage of co-cultivation, root
398 transcriptomics using control and *A. filiculoides* co-cultivated rice plants was assessed at 15 DAT via
399 RNA-seq analysis. The similarity between the gene expression profiles of the replicates of the same
400 treatment was assessed via PCA (FDR cut-off < 0.05) (Fig.4A). The dimensional-reduction analysis
401 revealed that the three replicates of R treatment clustered together as much as did those of R+Af
402 treatment. Among all annotated genes, 473 were differentially expressed (DE), of which 230 were
403 upregulated and 243 were downregulated (FDR cut-off = 0.05) (Fig 4B). The functional enrichment
404 analysis of the 473 DEGs at 15 DAT highlighted the 20 most enriched biological processes (BP) and
405 molecular function (MF) terms, shown in Fig 5A and B, respectively (FDR cut-off = 0.001 for both).
406 Notably, the methionine (Met) salvage pathway (MSP), the amino acids (aa) salvage pathway (ASP),
407 and iron and metal transport and homeostasis were the most enriched BP terms. As for MF, the terms
408 iron and metal binding and transmembrane transporters were the most enriched. No results were
409 obtained selecting the pathway database 'GO cellular component' (CC). Among the 230 upregulated
410 DE genes, the most enriched BP was intracellular sequestering of iron ion, whereas the response to
411 reactive oxygen species (ROS) was the BP with the highest number of genes (FDR cut-off = 0.001).
412 The most enriched MFs were ferric and ferrous binding (FDR cut-off = 0.001) (Fig. S4A and B). The
413 same analysis of the 243 downregulated DE genes revealed that the most enriched BPs were L-Met
414 recycling and iron and metal ions transport (FDR cut-off = 0.001), and the most enriched MF was
415 metal ions transport (FDR cut-off = 0.001) (Fig. S5 A and B).
416 The MSP is part of the cysteine and methionine metabolism, which also comprises the biosynthesis
417 of cysteine (M00021) and ethylene biosynthesis (M99368). Therefore, the MSP was further
418 investigated. All the DEGs involved in the pathway were downregulated (Table S3). Among the most

DE genes, those related to iron homeostasis were also included (Table S4). Rice employs two strategies for iron solubilization and uptake (Ishimaru *et al*., 2006, *Li et al.*, 2023), and genes related to both strategies were severely downregulated, whereas those for iron storage in plastids (*Ferritin 1*, *FER1, FC=2.45* and *ferritin 2*, *FER2, FC=2.49*) and vacuoles (*Vacuolar Iron Transporter 1*, *VIT1-2*, FC=6.07 and the *Vacuolar Iron Transporter Homolog 2*, *VITH2*, FC= 6.44) upregulated in the R+Af treatment (Fig.6, Table S4).
To investigate the link between iron homeostasis and methionine metabolism, a network analysis was performed by querying all DEGs (Fig. 7). The functional categories were linked if they shared ≥ 20% genes (FDR cut-off = 0.05). The results showed that the nodes – 'L-Met salvage pathway (MSP)' and 'iron homeostasis' – were connected to the node 'response to NO,' and are involved in response to stimulus, transport, and homeostasis of ions, in particular iron, and amino acid metabolism. Intriguingly, the terms L-Met salvage pathway, iron homeostasis, and response to NO shared a common gene, *Iron deficiency-induced protein 2 (IDI2)*, which was downregulated (FC= -3.32) in the presence of *A. filiculoides* (Table 1 and S3). Within the 15 DAT dataset, three NO-related genes were found to be upregulated: the *Nitrate reductase 2* (*NR2*), which encodes the NO biosynthetic enzyme, and two *Nitrate transporter (NRT)* genes (Table 1).

In the roots of *A. filiculoides* co-cultivated rice plants the higher levels of NO and *FER* mRNAs at 15 DAT were coupled with the upregulation of several genes coding for ROS scavengers such as *Catalase A1* (*CATA1,* FC=2.23), *Ascorbate peroxidase 1* (*APX1,* FC=1.60)*, Ascorbate peroxidase 7* (*APx7,* FC=.46)*,* the *Glutaredoxin-like protein 4* (*GRL4*, FC=1.77) and the *gluthatione transferase 41* (*GSTU41,* FC= 1.77) **(**Table S5).

Since R+Af treatment induced a differential accumulation pattern of the bioactive forms of IAA, ABA, CKs and SA (see below), the dataset was analysed for phytohormone-related genes (Table S6). The identified DEGs were generally not connected to the biosynthesis of these phytohormones, rather to their signalling and response. In this respect, it is noteworthy the differential regulation of 4 auxin -(*Os01g0924966*, FC=6,43; *Os09g0545400*, FC=-1,14; *Os09g0133200*, FC=-1,02; *Os09g0133200*, FC=-1,02985), 3 ABA - (*Os02g0543000*, FC= 3,333083; *Os11g0167800*, FC= 1,109878; *Os02g0734600*, FC= 1,491478), along with 2 CKs - (*Os04g0442300*, FC=2,17; *Os12g0139400*, FC=2,33) responsive genes. In particular, *Indole-3-Butyric Acid response 1 (IBR1, Os09g0133200*) involved in the conversion of the auxin precursor IBA to active IAA (Frick and Styrader, 2018) was downregulated (FC=-1,02), whereas the *Gretchen Hagen 3.12* (*GH3.12*, *Os11g0186500*), belonging to a family that catalyzes the conjugation reactions of salicylic acid, jasmonic acid, and IAA with amino acids to control their homeostasis (Guo et al., 2022), was upregulated (FC=3.43). Two ethylene-responsive genes (*Os04g0549800*, FC=3,70; *Os02g0656600*, FC=1,36) were upregulated in rice roots from R+Af treatment. Conversely, SA-related genes were not differentially expressed (Table S6).

Targeted qRT-PCR analysis validated and extended RNAseq results

To validate RNA-seq results at 15 DAT, and simultaneously investigate gene expression at earlier time points, the quantification of the expression of a subset of DEGs of interest was performed on rice roots from R+Af and R treatments by qRT-PCR (Table S1) sampled at 0, 5, 9, 12 and 15 DAT. Genes were selected according to their biological function and the expression levels in the RNA-seq dataset. Transcriptomics and qRT-PCR results were in good agreement. In fact, the significantly different expression of 10 out of the 12 genes tested by qRT-PCR at 15 DAT was confirmed. For the remaining 2 DEGs, the *basic Helix-Loop-Helix 58* (*bHLH58*) and the *Protein Phosphatase 2C* (*PP2C*), qRT-PCR analysis confirmed the higher levels of their mRNAs in the presence of *A. filiculoides*, although the increments in the expression were not significant (Fig. 8).

468 Overall, the qRT-PCR analysis showed that the differential expression of the selected DEGs was
469 evident much earlier than at 15 DAT. This occurred for the genes related to iron uptake/homeostasis
470 (*FER1*, *FER2*, *VIT1-2*, *TOM1*, *YSL2*, *IDI2*, *IDI4*), with two of them, namely *FER2* and *IDI4*,
471 differently expressed since 5 DAT, as well as for the gene related to NO biosynthesis (*NR*, since 9
472 DAT) and hormone maturation/signalling (*PP2C* at 12 DAT; *abscisic acid- stress- and ripening gene*
473 *3 -ASR3,* since 9 DAT and *GH3* since 9 DAT).

474

475 *Targeted-hormonomics in rice organs and growth media in the presence and absence of* A.
476 filiculoides
477
478 To evaluate whether the morphological and transcriptional changes determined in rice by *A.*
479 *filiculoides* could be related to an altered balance of phytohormones, the accumulation profiles of
480 phytohormones, along with that of their precursors and metabolites, were evaluated in the roots and
481 leaves of rice grown with and without *A. filiculoides* at 15 DAT. Furthermore, by assessing the
482 phytohormonal contents in the growth media of rice grown under the two treatments, we aimed to
483 gain insights into the molecular interplay occurring between *A. filiculoides* and rice. In Table S7, the
484 hormonal compounds investigated are given.
485
486 *The presence of Azolla altered the levels of hormones in rice roots and leaves*

487 Rice roots were sampled at 0 DAT (T_0) before rice experienced the hydroponic cultivation and at 15
488 DAT under R+Af or R treatment. Discriminant Analysis (sPLSDA) showed a clear separation
489 between roots from R and R+Af samples at 15 DAT (Fig. S6A). Additionally, the correspondent
490 sPLSDA loadings plot highlighted the compounds that contributed most to explaining the differences
491 between the treatments. The top ten compounds are reported in Fig. S6B and among them the most
492 relevant was iP7G, followed by ABA.
493
494 At 15 DAT the levels of 5 out of the 48 quantified compounds were significantly different in the R +
495 Af compared to the R treatment (Fig. 9, Table S8). These compounds belong to the cytokinin (CK),
496 ABA, auxin and phenolic classes. The levels of three of them, namely ABA, the phytoalexin DPA,
497 which is the product of irreversible ABA oxidation (Mongrand *et al*., 2003), and IAA-Glu were
498 significantly higher in the R+Af treatment. Conversely, iP7G and the phytoalexin SinAc contents
499 were significantly lower. At this time point, DZ9G was detected differently from 0 DAT, although
500 its levels were not different between treatments. By filtering the data less stringently, the levels of
501 two other compounds, cZROG and IAA-Asp, were significantly higher in R+Af at 15 DAT (unpaired
502 two samples t-test, $P < 0.05$; Table S8).

503 Looking at the root hormonal profiles from 0 to 15 DAT, it emerged that the presence of *A. filiculoides*
504 changed the accumulation profiles of several bioactive and metabolic forms in rice roots. In Table S9
505 the levels of all compounds detected in the R and R+Af treatments are given, whereas Fig 10 shows
506 the accumulation profiles of the bioactive forms. Among the bioactive forms, ABA levels increased
507 from 0 to 15 DAT in both treatments, but their levels were significantly higher in the R+Af vs R
508 treatment at 15 DAT (Fig. 10A).

509 Moving rice seedlings to hydroponic conditions caused a marked SA decrement and increased JA
510 root contents, irrespective of treatment. A more complex picture emerged for the bioactive CKs: the
511 levels of cZ did not decrease significantly at 15 DAT, whereas those of DZ did in both treatments.
512 Conversely, the accumulation of tZ at 15 DAT increased slightly in the presence of *A. filiculoides*,
513 but significantly in the control. Differently, iP levels increased significantly at 15 DAT, regardless of
514 the treatment (Fig. 10A).

515 For what concerns leaves, the sPLSDA analysis displayed a marked separation of the hormonal
516 compounds between R + Af and R treatments (Fig. S7A), with the oxidized forms of IAA, SA, and
517 several CKs being the compounds that contributed the most to their separation (Fig. S7B). Of the 50
518 quantified compounds in rice leaves at 15 DAT, 19 significantly differed between the treatments (Fig.
519 S8). In particular, among CKs, with the only exception for DZR, all the others (tZOG, DZOG, cZOG,
520 cZROG, iPRMP) were accumulated at higher levels in the presence of *A. filiculoides* (Table S10).
521 Under this condition, the 4 and 5 differentially accumulated ABA-related (ABA, ABA-GE, PA and
522 9OH-ABA) and IAA-related (IAA, IAA-Glu, IAM, I3A and ILacA) compounds, respectively, also
523 showed higher levels. Likewise, the levels of 3 phenolic compounds (SA, BzA and PAAM) and the
524 sole gibberellin detected (GA19) were higher in the presence of *A. filiculoides* (Fig. S8). By filtering
525 the data less strictly, the accumulation of 10 additional compounds was significantly different. These
526 were tZRMP, DZ, cZRMP, with lower levels and iP7G, iP9G, MeS-ZR, MeS-iP, DPA, JA-Me and
527 OxIAA-GE with higher levels (unpaired two samples t-test; $P < 0.05$; Table S10) in the R+Af vs R
528 treatment. By looking at the hormonal levels over time, it emerged that the presence of *A. filiculoides*
529 changed those of several bioactive (Fig 10B) and metabolic forms (Table S11) in rice leaves. Among
530 the bioactive forms, ABA and SA peaked at 15 DAT in both treatments, but their levels at this time
531 point were higher in the R+Af than in R treatment. IAA and JA levels decreased at 15 DAT, but the
532 decrement of IAA was significantly lower in the R+Af than R treatment. Among CKs, cZ and iP
533 decreased at 15 DAT in both treatments. The levels of DZ and tZ increased moving from 0 to 15
534 DAT, with DZ levels being higher in R than (in) R+Af treatment at 15 DAT (Fig. 10B).
535
536 A. filiculoides *and its symbiont released hormonal compounds in the media*
537
538 *A. filiculoides* affected the contents of the hormonal compounds in the media as significant differences
539 emerged between R and R+Af treatments at 15 DAT (Fig. S9A). Notably, among the compounds that
540 contributed to their separation, there were the phenolics PAAM and SA, along with several auxins,
541 CKs, and GA19 (Fig S9B).
542 Four of the 35 quantified compounds at 15 DAT were significantly different between the R + Af and
543 R media. Three of these compounds, iP9G, OxIAA and OxIAA-Asp, showed significantly higher
544 levels in the R+Af medium, while the levels of SA significantly decreased (Table S12 and Fig. S10).
545 To test the hypothesis that *T. azollae* provided some of the phytohormonal compounds detected in
546 the R + Af medium, phytohormone levels were assessed in the *T. azollae* (Ta) medium after 7 days
547 of growth and compared to the control medium, to which no exogenous hormones were added. The
548 analysis revealed that, in the Ta medium, 4 compounds, namely the CKs iP, cZ and DZOG, and the
549 auxin OxIAA-Glu accumulated (Fig. S11).
550
551
552 **Discussion**

553 A. filiculoides *alters the patterns of RSA and the aerial organ development in rice*

554
555 RSA plasticity is a significant trait enabling plants to cope with abiotic stress (Lavenus *et al*., 2013).
556 Understanding the effectors controlling this trait is therefore crucial to optimizing resource use by
557 crops in a more efficient and sustainable way. The present study shows *A. filiculoides* as a potent
558 trigger of RSA plasticity in rice. A divergent root architecture between co-cultivated and control rice
559 plants becomes in fact macroscopically apparent at 30 DAT, when *A. filiculoides* co-cultivated rice
560 plants show more and shorter ARs than control plants. These changes in AR patterning coincide with
561 a higher number of LRs. The dynamics of root development change with time because at 60 DAT,

562 the ARs of co-cultivated rice become significantly longer and slightly more numerous than those of
563 the control. Thus, *A. filiculoides* shapes the growth and spatial organization of rice roots. Likely, the
564 different RSA exhibited by rice plants in the presence of *A. filiculoides* optimizes nutrient uptake and
565 metabolite exchange between rice and the surrounding aqueous environment.

566 Co-cultivated rice plants also show increased height and number of tillers from 14 and 21 DAT,
567 respectively. From 28 DAT, the number of leaves is significantly higher in co-cultivated rice.
568 Notably, this number remains higher until the last sampling time point (63 DAT). A higher leaf
569 number in Azolla co-cultivated rice plants was also recently reported by Bazihizina et al. (submitted)
570 after 60 days of hydroponic condition. The same study also reported on a higher fresh shoot biomass
571 and shoot-to-root ratio at this time point in the presence of Azolla. Conversely, under our
572 experimental condition, the rice fresh aerial biomass was significantly higher at 30 DAT when it was
573 also significant the decrease of the root/shoot ratio in R+Af vs R treatment. It is likely that the
574 different experimental set up between present and Bazihizina et al.'s study results in a different timing
575 of rice organ development.

576 Overall, the present study provides an in-depth analysis on the morphogenic effects that co-cultivated
577 *A. filiculoides* exerts on rice over its early phases of vegetative growth. Because of the experimental
578 set up pursued in the present study, we can also conclude that these effects do neither result from the
579 inorganic nitrogen nor from the VOCs released by the fern. By replacing the growth media frequently
580 and employing only actively growing *A. filiculoides* plants, the content of inorganic nitrogen available
581 to rice co-cultivated plants did not increase compared to the media in which rice plants were grown
582 alone. Yet, *A. filiculoides* co-cultivated and control rice plants were grown side by side in the same
583 growth chamber to allow the VOCs emitted by the fern to diffuse freely among rice plants, regardless
584 of the treatment.

585 *RSA changes are preceded by a boost of NO and differential expression of iron related genes at 15*
586 *DAT*
587
588 The changes in RSA seen in rice plants co-cultivated with *A. filiculoides* at 30 DAT imply metabolic
589 and molecular changes that occurred at earlier time points. NO, a highly reactive redox signalling
590 molecule, is a central co-regulator in many growth and developmental processes (Qiao and Fan, 2008;
591 Yu *et al.*, 2014; Sánchez-Vicente, *et al.*, 2019), including the induction and formation of AR and LR
592 (Geiss *et al.*, 2009; Xiong *et al.*, 2009; Correa-Aragunde *et al.*, 2016). Similarly, the reactive nitrogen
593 species (RNS) and ROS signaling molecule network, in synergy with hormonal signaling pathways,
594 control RSA (Prakash *et al.*, 2020). The changes in rice RSA observed at 30 DAT are preceded at 15
595 DAT by a significant increase of NO contents and differential regulation of almost 500 genes in the
596 roots. The GO analysis of DEGs unveiled the commitment of different molecular pathways in
597 response to *A. filiculoides*, and a network hub made up of the S-adenosylmethionine cycle, response
598 to iron, and response to NO (Fig. 7). Thus, transcriptomic data are consistent with the biochemical
599 evidence of higher NO levels at 15 DAT in the roots of rice co-cultivated with *A. filiculoides*.

600 NR is the most critical source of $NO^{\cdot}$ in plants, and the nitrate concentration/availability in the rooting
601 medium can affect the amount of NO via mediation of NO synthase (NOS) and $NO^{\cdot}$ reductase (NR)
602 activity (Yamasaki *et al.*, 1999; Meyer *et al.*, 2005; Yamasaki, 2005; Zhao *et al.*, 2007) and hence
603 growth. According to Sun and colleagues (2015), NO generated by the NR pathway by increasing LR
604 initiation and the inorganic N uptake rate may represent a strategy for rice plants to adapt to a
605 fluctuating nitrate supply. In keeping with the biochemical quantification of $NO^{\cdot}$ in the roots of co-
606 cultivated rice, genes involved in $NO^{\cdot}$ biosynthesis, *NR2*, and nitrate uptake, such as *NRT1.1B,* were
607 significantly upregulated at 15 DAT, as was the *nitrate and chloride transporter NRT* (Table 2).
608 Additionally, *NR* upregulation was significant from 9 DAT as shown by qRT-PCR analysis. In

609 Arabidopsis *NRT1.1B* plays multiple roles, one of which is as auxin transporter at low nitrate
610 concentrations (Krouk *et al*., 2010; Forde, 2014). Recently, *NRT1.1B* was found to promote root-to-
611 shoot nitrate translocation and *NRT1.1-NR2* overexpression to improve NUE (Gu and Yang, 2022).
612 The upregulation of *NRT1.1B* in the roots of *A.filiculoides* co-cultivated plants cannot be explained
613 by an increase of nitrate content in the medium. This observation sets the stage to future investigations
614 aimed at identifying additional triggers of *NRT1.1B* regulation. There might be other nitrogen sources
615 present in the media or the different hormonal profiles exhibited by the roots of *A. filiculoides* co-
616 cultivated plants. In this context, we observed that in the presence of the fern, the levels of organic
617 nitrogen in the media, such as small peptides and amino acids, as shown in the companion paper by
618 Consorti *et al*. (preprint), and those of hormones such as auxin and ABA (see below) increased. Yet,
619 NO· and ABA are interlocking molecules that can exert a combined effect on expression profiles of
620 key genes involved in N-uptake and translocation under stress (Sahay *et al*., 2021).
621
622 The regulation of Fe homeostasis is among the key roles of NO (Tewari *et al*., 2021). The effects of
623 NO on Fe homeostasis have been mainly investigated in relation to Fe deficiency, a condition that
624 induces the upregulation of genes for Fe uptake. However, from our transcriptomics data emerged
625 downregulation of such genes. Fe plays a significant role in determining RSA. The availability and
626 uptake of iron have an impact on primary and LR growth and root hair development thereby inducing
627 RSA plasticity (Muller and Schmidt, 2004; Li *et al*., 2016). Also, alternating wet and dry periods in
628 the irrigation of rice leads to the alternant occurrence of Fe deficiency and Fe excess during the rice
629 growth period (Zhang *et al.*, 2022). As a consequence, rice has developed a sophisticated mechanism
630 to enhance its Fe stress tolerance and cope with such situations. This mechanism is based on a
631 combination of the chelation-based strategy (Strategy II) and some features of the iron reduction-
632 based strategy (Strategy I) (Li *et al*., 2020). In strategy II, MA family phytosiderophores are
633 synthesized in vesicles and secreted out of the root to chelate Fe^{3+}. During the synthesis of DMA,
634 three sequential enzymatic reactions are catalyzed by nicotinamide (NA) synthase (NAS), NA
635 aminotransferase (NAAT), and deoxymugineic acid synthase (DMAS) (Li *et al*., 2020). NAS activity
636 depends on the availability of methionine, which links the S-methionine salvage pathway (MSP) to
637 iron absorption and homeostasis, as it emerged from the ShinyGO analysis (Figures 5, 7).

638 The MSP pathway is severely downregulated in co-cultivated rice roots. Within this pathway, which
639 is also important for the biosynthesis of isoprenoids and ethylene, the downregulation of *IDI2*
640 emerged from 9 DAT onwards and that of IDI4 from 5 DAT as per qRT-PCR data. After being
641 synthesized in root cells, DMAs are secreted into the rhizosphere by TOM1, whose gene is
642 downregulated in the presence of *A. filiculoides* from 9 DAT (Fig 8). The Fe^{3+}-DMA complexes
643 formed in the rhizosphere are transported into root cells by YSL proteins. The rice *YSL2* is
644 significantly downregulated from 9 DAT onwards (Fig.8). Despite preferentially being a strategy II
645 plant, rice also absorbs Fe^{2+} directly via IRTs. In the presence of *A. filiculoides*, both *IRT1* and *2* are
646 severely downregulated at 15 DAT (Table S4). Rice compartmentalizes excessive Fe as ferritins or
647 in vacuoles by inducing the expression of *FER*s and *VITs,* respectively (Zhang *et al.*, 2022). Not only
648 *FER1* and *FER2* but also *VIT1-22* and *VITH2* are upregulated in the presence of *A. filiculoides* (Table
649 S4). *FER1* is upregulated from 9 DAT, while *FER2*, the highest expressed ferritin of the two, from 5
650 DAT onwards (Fig 8). The expression of *FERs* in rice can depend on metals and oxidative stress
651 (Stein *et al*., 2009). In maize *FER2* is regulated through an ABA-dependent pathway whereas *FER1*
652 requires NO and iron through an ABA-independent pathway (Petit *et al*., 2001). We note that both
653 NO and ABA levels are increased in *A. filiculoides* co-cultivated rice roots at 15 DAT. The expression
654 patterns of genes involved in iron absorption, homeostasis, inclusion and sequestration emerged in
655 the present study nicely overlap with those in the roots of rice grown in hydroponics for 14 days under
656 different levels of iron excess (Aung *et al*., 2018). This suggests that *A. filiculoides* co-cultivated rice
657 plants experience a condition of iron excess. However, the increased bioavailability of iron in the

presence of *A. filiculoides* seems not to reach toxic levels in rice since no specific morphological symptoms of excess iron, such as bronzing of leaves and roots and stunted roots, occurred.

The downregulation of genes for siderophore biosynthesis in the roots of *A. filiculoides* co-cultivated rice plants might imply that these plants rely on the siderophores released into the medium by the cyanobacteria hosted in the fronds of *A. filiculoides* for iron uptake. Cyanobacteria produce siderophores (Singh, 2014; Chakraborty *et al*., 2019) and those hosted in *Azolla* fronds could make iron and other nutrients more bioavailable in the medium.

Due to the higher iron and nitrate contents in rice roots, a robust generation of ROS (Nguyen *et al.*, 2022) and RNS (Tewari *et al*., 2021; Kirk *et al.*, 2022) is induced, and various detoxification responses are activated (Aung *et al.*, 2018), so plants can quickly adjust growth to the environment by influencing the cellular redox state and signalling (Yuan *et al.*, 2013). The significantly higher content of NO also modulates the antioxidant system. In our system, we found the upregulation of several genes involved in the antioxidant system (Table S5) in the roots of *A.filiculoides* co-cultivated plants at 15 DAT.

A. filiculoides *induces changes in phytohormone levels in rice roots and growth media*

The morphological differences in root patterning along with the evidence that among the DEGs at 15 DAT there are genes related to phytohormone signalling prompted us to analyse the phytohormone levels in rice roots, as well as the hormones present in the cultivation media of rice grown with and without *A. filiculoides*, and those likely supplied by the Azolla symbiont *T. azollae*.

Among the metabolites quantified, only 7 are differentially accumulated between rice roots from R and R+Af treatments at 15 DAT. The levels of two of them, the CK iP7G and the phytoalexin sinAC decreased, while those of the ABA, cZROG, DPA, IAA-Glu and IAA-Asp significantly increased in the presence of *A. filiculoides*. The high levels of ABA in the roots of rice co-cultivated with *A. filiculoides* at 15 DAT is noteworthy. ABA activity is associated, downstream of ethylene action and along with ROS, to ARs initiation in rice (Mhimdi and Pérez-Pérez, 2020). This occurs under waterlogging conditions and directly depends on the continuously produced auxin in the shoot, which is transported through the stem to the roots (Mhimdi and Pérez-Pérez, 2020). Notably, AR and LR initiation and growth are the most noticeable morphological changes exhibited by rice roots in the presence of *A. filiculoides.* In keeping with the increased levels of ABA, there is the upregulation of three ABA responsive genes (*ASR*s) (Table S6). The qRT-PCR analysis showed that *ASR3*, the most highly expressed *ASR*, is upregulated not only at 15 DAT, but also at earlier time points, 9 and 12 DAT (Fig. 8). This finding suggests that the ABA contents increase in rice roots occurred earlier than at 15 DAT. Also, the upregulation of two supposedly negative regulators of the ABA response genes, *PP2C30* and *PP2C27* (Table S6), may indicate a need to control or reduce the effects of ABA to regulate the RSA. In line with this observation, among other differentially expressed *WRKYs*, the marked upregulation of *WRKY40* (FC= 4.20, Table S6) at 15 DAT is noteworthy. In *A. thaliana* this gene is rapidly induced by ABA and acts as a transcriptional repressor of ABA response (Chen *et al.*, 2010).

It is generally assumed that CKs act as shoot growth-promoting factors and negative regulators of root development. For instance, exogenous cytokinin treatments inhibit root elongation, but increase plant height and nutrient contents in aerial organs (Beemster and Baskin, 1998; Zahir *et al*., 2001). CKs also inhibit genes related to iron absorption and homeostasis such as *IRT1, FRO2* and *FIT* (Séguéla *et al.*, 2008; Gao *et al.*, 2019). Thus, along with the supply of siderophores, the provision of CKs by *A. filiculoides* could explain the downregulation of rice genes for iron uptake and the changes in RSA. Yet, the competence of *T. azollae* and its host to synthesize and release CKs in the media coupled with the evidence that genes for CKs biosynthesis are not differentially expressed in rice

704 roots, lead us to argue that rice roots might indeed perceive and even metabolizes exogenous CKs
705 (Zahir *et al*. 2001). Along this reasoning, we note the upregulation of two key genes in CK signaling,
706 the *A-type response regulators RR1* (FC= 2.17) and *RR10* (FC= 2.33) in the roots of *A. filiculoides*
707 co-cultivated plants (Table S6). Genes of G subfamily ATP-binding cassette (*ABCG*) code for CK
708 transporters. In rice only the *OsABCG18* has been characterized as involved in long-distance transport
709 of CKs thus far (Zhao *et al.*, 2019). The upregulation of another a *ABCG transporter*, *Os01g0836600*
710 (FC= 2.6,Table S6) in the roots of *A.filiculoides* co-cultivated rice plants paves the way for future
711 research to assess whether this gene could be added to the CKs transporters.

712 Many aspects of LR formation from priming to emergence are controlled by auxins (Lavenus *et al*.,
713 2013). Although the concentration of IAA increases only slightly in the roots of *A. filiculoides* co-
714 cultivated rice at 15 DAT, that of its storage forms increases significantly. Thus, the presence of the
715 fern impacts on the homeostasis of this hormone. The upregulation at 15 DAT of *NRT1.1,* might
716 concur to shape rice RSA via re-distribution of auxin. This goes along with the marked increase of
717 the auxin responsive gene, *small auxin-up RNA 3* (*SAUR3;* FC = 6.43) and the auxin transporter,
718 *ABCB* (FC = 1.75) (Table S6). Auxin homeostasis is partly sustained by the *GH3* gene family, which
719 can be seen as supervisors of the fluctuation of auxin levels. Although evidence for its function is
720 missing, the increase of the *GH3.12* mRNA levels from 9 DAT onwards may suggest its involvement
721 in the conjugation of amino acids to IAA, so explaining the increase of the IAA storage from IAA-
722 Glu at 15 DAT (Fig 10).

723 Ethylene is a hormone that plays a vital role in regulating RSA, by acting together with auxin and
724 other phytohormones (Růžička *et al.*, 2007; Carvalho *et al*., 2015). We have not quantified the levels
725 of ethylene, however, since two genes involved in ethylene response, *ERF32* (FC = 1.36) and *ERF37*
726 (FC = 3.70), are overexpressed (Table S6), we can infer that the presence of *A. filiculoides* may induce
727 the ethylene signaling pathway in rice roots.
728
729 Although no differences in SA levels emerged in the roots of control and *A. filiculoides* co-cultivated
730 plants, their levels decrease in the R+Af media. This observation goes along with the capacity of
731 aquatic organisms such as *Azolla* and *Lemma* spp. to uptake SA and other organic compounds from
732 the media (Maldonado *et al*., 2022) and with the observation that, although some of the key genes for
733 SA biosynthesis seem to be absent in its genome, *A. filiculoides* is responsive to exogenously applied
734 SA (de Vries *et al*., 2018). Being SA a key hormone in plant immunity, lower levels of SA in the
735 medium may indicate that co-cultivation with *A. filiculoides* can perturb the capability of rice or of
736 both plants to interact with each other and with the environment.
737

738 *The boost in the development of rice aerial organs reflects the perturbation in the hormonal content*
739 *in leaves of Azolla co-cultivated rice plants*

740 The morphological changes of aerial organs of *A. filiculoides* co-cultivated plants seem to precede
741 those occurred in roots. Number of leaves, plant height and number of tillers are in fact significantly
742 higher in co-cultivated rice vs control plants well before 30 DAT, when differences in the RSA pattern
743 emerged. However, the differentiation of more organs (tillers and leaves) and, more interestingly, the
744 increase in plant height, seen since 14 DAT, are not sustained at the expenses of root biomass, at least
745 up to 30 DAT. Once again, signal exchanged at root levels between the two partners might have
746 concurred to a different balance of regulators in the first stage of rice aerial organ development. The
747 higher levels of auxins, either bioactive, precursor and storage forms, and of the GA precursor GA19,
748 in the leaves of *A. filiculoides* co-cultivated rice plants suggest this is indeed the case. Auxins in fact
749 promote leaf cell elongation and cell division at leaf node, resulting in an increase in the leaf pitch
750 and gibberellins have a central role in determining leaf growth and height (Zhao *et al*., 2021;
751 Sprangers *et al.*, 2020). While the levels of bioactive CK forms do not increase in the leaves of *A.*

752 *filiculoides* co-cultivated vs to control rice plants, those of the CK precursor, transport and storage
753 forms are higher. Thus, in the presence of *A. filiculoides* the homeostasis of CKs in rice leaves is
754 perturbed. Because CKs regulate the expression of nitrogen transporters from old to new leaves (Kiba
755 *et al*., 2011), it would be interesting to assess whether the gradient of nitrogen distribution in rice
756 canopy changes following co-cultivation with *A. filiculoides*.
757
758 In the leaves of *A. filiculoides* co-cultivated plants the levels of ABA are also higher. ABA is known
759 to affect mainly seed dormancy and germination, stomatal closure and stress tolerance. However, the
760 evidence that ABA-deficient mutants in *A. thaliana* show smaller plant stature and leaf growth than
761 wild type suggests that endogenous physiological concentrations of ABA may act as growth
762 promoter. In line with this, these mutants exhibit reduced cell area and cell number (Horiguchi *et al*.,
763 2006; Barrero *et al*., 2005), while in wild type *A. thaliana* plants ABA maintains shoot development
764 and leaf expansion in well-watered plants (LeNoble *et al*., 2004). It is therefore conceivable that as
765 in *A. thaliana* ABA also has a dual function in rice: growth inhibitor under stress and growth promoter
766 under controlled conditions (Cheng *et al*., 2002).
767
768 Besides its function during biotic and abiotic stress, SA plays a crucial role in the regulation of
769 physiological and biochemical processes during the entire lifespan of the plant (Rivas-San Vicente
770 and Javier Plasencia, 2011). Although a combination of several internal and external stimuli
771 contributes to plant growth and development, it was shown that micromolar application of SA to
772 seedling/ plantlet shoots of different species increases stem diameter, leaf number and fresh biomass
773 (Tucuch-Haas *et al*., 2017). Thus, by affecting leaf and chloroplast structure, SA is an important
774 regulator of photosynthesis. As an example, the photosynthetic rate is increased in maize sprayed
775 with 10−2M SA (Khodary, 2004). In turn, it is likely that the higher levels of SA detected in the
776 leaves of Azolla co-cultivated plants might sustain a higher photosynthetic rate and, in turn, the higher
777 areal biomass observed at 30 DAT. Moreover, the higher levels of SA in *A. filiculoides* co-cultivated
778 plants leaves let us argue that treated plants could cope better with stress than control plants.
779
780
781 **Conclusions**
782
783 Here we show for the first time the morphogenic effects that *A. filiculoides* exerts on rice plants at
784 the early phases of co-cultivation. The alteration in the development program triggered by the fern
785 on rice plants reflects and likely results from the increased availability in the co-cultivation medium
786 of small peptides, lipids and flavonoids, as shown in the companion paper by Consorti *et al*. (preprint),
787 as well as from the change in hormonal balance in rice roots and leaves, and an increased availability
788 of mineral nutrients. The present study shows in fact that *A. filiculoides* and its symbiont *T. azollae*
789 are competent to release in the liquid medium CKs and storage forms of auxins that are likely
790 transduced and metabolized by rice roots. Moreover, although the presence of *A. filiculoides* induces
791 the upregulation of rice root genes for iron sequestration and compartmentalization, as it occurs when
792 plants experience iron toxicity, co-cultivated rice plants do not show symptoms of iron excess. No
793 lastly, the co-cultivation with *A. filiculoides* induces an increase in SA levels in rice leaves. This
794 observation, along with enhanced formation of ARs and the boost in the development of the above-
795 ground organs in rice seedlings, point towards the co-cultivation with *A. filiculoides* as a sustainable
796 strategy to help rice plantlets coping with abiotic and biotic stress. Thus, future investigations will be
797 carried out for assessing how and to what extent Azolla co-cultivation impacts rice plant development
798 and seed yield under stressful conditions. Finally, the present study highlights a metabolic hub in
799 which different hormones and increased levels of iron and NO likely play a major role in determining
800 a more efficient rice RSA. The employment of rice mutants, impaired in the biosynthesis and

perception of these compounds, and different rice varieties, will allow us to understand more about the intricate below-ground metabolic crosstalk taking place between Azolla and rice.

Acknowledgments

This work is dedicated to the memory of our eminent colleague Stefania Pasqualini who conceived this study, earned a grant that supported it, and supervised the doctoral research activity of S.C. We thank Agnese Bertoldi for her hep with plant growth and sampling.

Author contributions

FP and MK designed the study; SC and AC carried out the entire experimental set. SC, AC, MC and LR performed morphological analysis. SC, CP, MCV, VG, GCZ, PID, MMK and FP performed molecular analyses. LR, PID, MMK and FP supervised the study. SC, LR and FP wrote the manuscript with the contribution of all the authors.

Conflict of interest

No conflict of interest declared.

Funding

This research was supported by PRIN project 2017 (Prot.2017N5LBZK): "A multidisciplinary approach to gain sustainable improvement of rice productivity through the co-cultivation with the fern Azolla and its cyanobacterial symbiont" financed by the Italian Ministry of Research (MUR) and, partially, by TowArds Next GENeration Crops Project, reg. no. CZ.02.01.01/00/22_008/0004581 of the ERDF program Johannes Amos Comenius. MCV was funded by "ON Foods" - Research and innovation network on food and nutrition Sustainability, Safety and Security – CUP B83C22004790001" project.

Data availability

The RNAseq data are available in the NCBI Gene Expression Omnibus database (https://www.ncbi.nlm.nih.gov/geo), accession number GSE278294. All other relevant data can be found within the manuscript and its supplementary data online.

References

Alexandratos N, Bruinsma J. 2012. World agriculture towards 2030/2050. The 2012 Revision Proof Copy', ESA Working paper (FAO), 12, pp. 1–154. https://ageconsearch.umn.edu/record/288998%0Ahttp://www.fao.org/economic/esa.

Andrews S. 2021 FastQC, A quality control tool for high throughput sequence data. https://www.bioinformatics.babraham.ac.uk/projects/fastqc

Aronesty E. 2011. 'Ea-utils: command-line tools for processing biological sequencing data'. https://github.com/ExpressionAnalysis/ea-utils

Aung MS, Masuda H, Kobayashi T., Nishizawa NK. 2018. Physiological and transcriptomic analysis of responses to different levels of iron excess stress in various rice tissues. Soil Science and Plant Nutrition 64(3), 370–385. doi:10.1080/00380768.2018.1443754

Banach A, Kuźniar A, Mencfel R, Wolińska A. 2019. The study on the cultivable microbiome of the aquatic fern Azolla filiculoides L. as new source of beneficial microorganisms. Applied Sciences 9, 1–20. doi: 10.3390/app9102143

Barrero JM, Piqueras P, González-Guzmán M, Serrano R., Rodríguez PL, Ponce MR, Micol JL. 2005. A mutational analysis of the ABA1 gene of Arabidopsis thaliana highlights the involvement of ABA in vegetative development. Journal of Experimental Botany, *56*(418), 2071–2083. doi: 10.1093/jxb/eri206

Beemster GTS, Baskin TI. 1998. Analysis of cell division and elongation underlying the developmental acceleration of root growth in Arabidopsis thaliana. Plant Physiology 116, 1515–1526. doi: 10.1104/pp.116.4.1515.

Bhuvaneshwari K, Singh PK. 2015. Response of nitrogen-fixing water fern Azolla biofertilization to rice crop. 3 Biotech *5*(4), 523–529. doi: 10.1007/s13205-014-0251-8

Bizzarri M, Delledonne M, Ferrarini A, Tononi P, Zago E, Vittori D, Damiani F, Paolocci F. 2020. Whole-Transcriptome Analysis Unveils the Synchronized Activities of Genes for Fructans in Developing Tubers of the Jerusalem Artichoke. Frontiers in Plant Science *11*, 1–22. doi: 10.3389/fpls.2020.00101

Brilli F, Srikanta Dani KG, Pasqualini S, Costarelli A, Cannavò S, Paolocci F, Chini Zittelli G, Mugnai G, Baraldi R, Loreto F. 2022. Exposure to different light intensities affects emission of volatiles and accumulations of both pigments and phenolics in Azolla filiculoides. Physiologia Plantarum 174(1), 1–16. doi: 10.1111/ppl.13619

Carvalho LC, Vidigal P, Amâncio S. 2015. Oxidative stress homeostasis in grapevine (Vitis vinifera L.). Frontiers in Environmental Science 3. doi: 10.3389/fenvs.2015.00020

Casanova D, Goudriaan J, Forner MMC, Withagen JCM. 2002. Rice yield prediction from yield components and limiting factors. European Journal of Agronomy 17(1), 41–61. doi: 10.1016/S1161-0301(01)00137-X

Chakraborty S, Verma E, Singh SS. 2018. Cyanobacterial Siderophores: Ecological and Biotechnological Significance. In Cyanobacteria: From Basic Science to Applications. Elsevier Inc. https://doi.org/10.1016/B978-0-12-814667-5.00019-2

Chen H, Lai Z, Shi J, Xiao Y, Chen Z, Xu X. 2010. Roles of Arabidopsis WRKY18, WRKY40 and WRKY60 transcription factors in plant responses to abscisic acid and abiotic stress, BMC Plant Biology 10, 1–15. doi: 10.1186/1471-2229-10-281

Cheng WH, Endo A, Zhou L. 2002. A unique short-chain dehydrogenase/reductase in arabidopsis glucose signaling and abscisic acid biosynthesis and functions. Plant Cell 14(11), 2723–2743. doi: 10.1105/tpc.006494

Consorti E, Costarelli A, Cannavò S. et al. Co-cultivation with Azolla affects the metabolome of whole rice plant beyond canonical inorganic nitrogen fertilization. BioRxive submitted

Correa-Aragunde N, Foresi N, Lamattina L. 2016. Auxin and nitric oxide: a counterbalanced partnership ensures the redox cue control required for determining root growth pattern. Advances in Botanical Research 77, 41–54. doi: 10.1016/bs.abr.2015.10.006

Costarelli A, Cannavò S, Cerri M, Pellegrino RM, Reale L, Paolocci F, Pasqualini S. 2021. Light and Temperature Shape the Phenylpropanoid Profile of Azolla filiculoides Fronds. Frontiers in Plant Science 12, 1–18. doi: 10.3389/fpls.2021.727667

Day PR. 1973. Genetic variability of crops. Annual Review of Phytopathology 11, 293–312. doi: 10.1146/annurev.py.11.090173.001453

de Castro Dos Santos FI, Marini N, dos Santos RS, Fernandes Hoffman B S, Alves-Ferreira M, de Oliveira AC. 2018. Selection and testing of reference genes for accurate RT-qPCR in rice seedlings under iron toxicity. PLoS ONE, 13(3). https://doi.org/10.1371/journal.pone.0193418

de Vries S, de Vries J, Teschke H, von Dahlen J K, Rose LE, Gould SB. 2018. Jasmonic and salicylic acid response in the fern Azolla filiculoides and its cyanobiont. Plant Cell and Environment 41, 2530–2548. doi: 10.1111/pce.13131

Escaray FJ, Passeri V, Babuin FM, Marco F, Carrasco P, Damiani F, Pieckenstain FL, Paolocci F, Ruiz OA. 2014. Lotus tenuis x L. corniculatus interspecific hybridization as a means to breed bloat-safe pastures and gain insight into the genetic control of proanthocyanidin biosynthesis in legumes. BMC Plant Biology 14. doi: 10.1186/1471-2229-14-40

Ewels P, Magnusson M, Lundin S, Käller M. 2016. MultiQC: Summarize analysis results for multiple tools and samples in a single report. Bioinformatics. 2016 Oct 1;32(19):3047-8. doi: 10.1093/bioinformatics/btw354.

Fogg GE, Stewart WDP, Fay P, Walsby AE. 1973. 'The blue-green algae', New York (USA): Academic Press, 460 pp

Food World Organization (FAO).2009a. 'Global agriculture towards 2050', High Level Expert Forum, Rome (Italy): FAO. http://www.fao.org/fileadmin/templates/wsfs/docs/Issues_papers/HLEF2050_Global_Agriculture.pdf.

Food World Organization (FAO). 2009b. 'How to Feed the World in 2050', Insights from an expert meeting at FAO, 2050, Rome (Italy): FAO. http://www.fao.org/wsfs/forum2050/wsfs-forum/en/.

Food World Organization (FAO). 2022a. 'Crop Prospects and Food Situation', Quarterly Global Report, Rome (Italy): FAO. doi: 10.4060/cc3233en.- 190 -

Food World Organization (FAO). 2022b. 'World Food and Agriculture - Statistical Pocketbook 2022', FAO, Rome (Italy): FAO. doi: 10.4060/cc2212en.

Forde BG. 2014. Nitrogen signalling pathways shaping root system architecture: An update. Current Opinion in Plant Biology 21, 30–36. Doi: 10.1016/j.pbi.2014.06.004

Frick EM, Strader LC. 2018. Roles for IBA-derived auxin in plant development. Journal of Experimental Botany 69(2), 169-177. doi: 10.1093/jxb/erx298

Gaillard MDP, Glauser G, Robert CAM, Turlings TCJ. 2018. Fine-tuning the "plant domestication-reduced defense" hypothesis: specialist vs generalist herbivores. New Phytologist 217, 355–366. doi: 10.1111/nph.14757

Gao S, Xiao Y, Xu F, Gao X, Cao S, Zhang F, Wang G, Sanders D, Chu C. 2019. Cytokinin-dependent regulatory module underlies the maintenance of zinc nutrition in rice. New Phytologist 224, 202–215. doi: 10.1111/nph.15962

Ge SX, Jung D, Yao R. 2020. ShinyGO: a graphical gene-set enrichment tool for animals and plants. Bioinformatics, 36(8), 2020, 2628–2629 doi: 10.1093/bioinformatics/btz931

Geiss G, Gutierrez L, Bellini C. 2009. Adventitious root formation. New insights and perspectives. In Annual Plant Reviews: Root Development; Beeckman, T (ed). Wiley-Blackwell: Oxford, UK, 127–156.

Godfray HCJ, Beddington JR, Crute IR, Haddad L, Lawrence D, Muir JF, Pretty J, Robinson S, Thomas SM, Toulmin C. 2010. Food security: the challenge of feeding 9 billion people. Science 327, 812–818. doi: 10.1126/science.1185383

Gregorio GB, Senadhira D, Mendoza RD. 1997. Screening rice for salinity tolerance. IRRI Discussion Paper Series No. 22. Manila (Philippines) lnternational Rice Research Institute.

Gu J, Yang J. 2022. Nitrogen (N) transformation in paddy rice field: Its effect on N uptake and relation to improved N management. Crop and Environment 1(1), 7-14. doi: 10.1016/j.crope.2022.03.003

Guo R, Hu Y, Aoi Y, Hira H, Ge C, Dai X, Kasahara H, Zhao Y. 2022. Local conjugation of auxin by the GH3 amido synthetases is required for normal development of roots and flowers in Arabidopsis. Biochemical and Biophysical Research Communications 589, 16–22. doi: 10.1016/j.bbrc.2021.11.109

Herath BM, Karunarathna SC. 2023. Azolla as the multifunctional fern in organic agriculture: Prospects and challenges: A Review Article. International Journal of Agricultural Technology 19(1): 63-82. http://www.ijat-aatsea.comhttps://www.researchgate.net/publication/367268446

Horiguchi G, Ferjani A, Fujikura U, Tsukaya H. 2006. Coordination of cell proliferation and cell expansion in the control of leaf size in Arabidopsis thaliana. Journal of Plant Research 119(1), 37-42. doi: 10.1007/s10265-005-0232-4

Ishimaru Y, Suzuki M, Tsukamoto T. 2006. Rice plants take up iron as an Fe^{3+}- phytosiderophore and as Fe^{2+}. Plant Journal 45(3), 335–346. doi: 10.1111/j.1365-313X.2005.02624.x

Jeong H, Park J, Kim H. 2013. Determination of NH_4^+ in environmental water with interfering substances using the modified nessler method. Journal of Chemistry. doi: 10.1155/2013/359217

Kar S, Panda SK. 2020. Iron homeostasis in rice: deficit and excess. Proceedings of the National Academy of Sciences India Section B - Biological Sciences 90, 227–235. doi: 10.1007/s40011-018-1052-3

Kawahara Y, de la Bastide M, Hamilton JP. 2013. Improvement of the Oryza sativa Nipponbare reference genome using next generation sequence and optical map data. Rice 6, 1–10. doi: 10.1186/1939-8433-6-1

Khodary SEA. 2004. Effect of Salicylic Acid on Growth, Photosynthesis and Carbohydrate Metabolism in Salt Stressed Maize Plants. International Journal of Agriculture and Biology, 6, 5-8.

Khumairoh U, Lantinga EA, Schulte RPO, Suprayogo D, Groot JCJ. 2018. Complex rice systems to improve rice yield and yield stability in the face of variable weather conditions. Scientific Reports 8, 1–10. doi: 10.1038/s41598-018-32915-z

Kiba T, Kudo T, Kojima M, Sakakibara H. 2011. Hormonal control of nitrogen acquisition: Roles of auxin, abscisic acid, and cytokinin. Journal of Experimental Botany 62(4), 1399–1409). doi: 10.1093/jxb/erq410

Kirk GJD, Manwaring HR, Ueda Y, Semwal V, Wissuwa M. 2022. Below-ground plant–soil interactions affecting adaptations of rice to iron toxicity', Plant Cell and Environment, 45, pp. 705–718. doi: 10.1111/pce.14199.

Kobayashi T, Itai RN, Nishizawa NK. 2014. Iron deficiencyresponses in rice roots. Rice 7:1–21. https://doi.org/10.1186/s12284-014-0027-0

Kojima H, Nakatsubo N, Kikuchi K, Kawahara S, Kirino Y, Nagoshi H, Hirata Y, Nagano T. 1998. Detection and imaging of nitric oxide with novel fluorescent indicators: diaminofluoresceins. Analytical Chemistry 70, 2446–2453. doi: 10.1021/ac9801723

Krouk G, Lacombe B, Bielach A, et al. 2010. Nitrate-regulated auxin transport by NRT1.1 defines a mechanism for nutrient sensing in plants. Developmental Cell 18, 927–937. doi: 10.1016/j.devcel.2010.05.008

Ladha JK, Dawe D, Ventura TS, Singh U, Ventura W, Watanabe I. 2000. Long-Term Effects of Urea and Green Manure on Rice Yields and Nitrogen Balance. Soil Science Society of America Journal 64(6), 1993–2001. doi: 10.2136/sssaj2000.6461993x

Lavenus J, Goh T, Roberts I, Guyomarc'h S, Lucas M, de Smet I, Fukaki H, Beeckman T, Bennett M, Laplaze L. 2013. Lateral root development in Arabidopsis: Fifty shades of auxin. Trends in Plant Science 18(8), 450-458. doi: 10.1016/j.tplants.2013.04.006

LeNoble ME, Spollen WG, Sharp RE. 2004. Maintenance of shoot growth by endogenous ABA: Genetic assessment of the involvement of ethylene suppression. Journal of Experimental Botany 55(395), 237–245. doi: 10.1093/jxb/erh031

Li B, Dewey CN. 2011. RSEM: Accurate transcript quantification from RNA-seq data with or without a reference genome. Bioinformatics 12, 1-16. doi: 10.1201/b16589

Li G, Kronzucker HJ, Shi W. 2016. The response of the root apex in plant adaptation to iron heterogeneity in soil. Frontiers in Plant Science 7, 1-7. doi: 10.3389/fpls.2016.00344

Li M, Watanabe S, Gao FF, Dubos C. 2023. Iron nutrition in plants: towards a new paradigm? Plants 12, 384. doi: 10.3390/plants12020384.

Li Q, Chen L, Yang A. 2020. The molecular mechanisms underlying iron deficiency responses in rice. International Journal of Molecular Sciences 21. doi: 10.3390/ijms21010043

Love MI, Huber W, Anders S. 2014. Moderated estimation of fold change and dispersion for RNA-seq data with DESeq2. Genome Biology 15, 1-21. doi: 10.1186/s13059-014-0550-8

Lumpkin TA, Plucknett DL. 1980. Azolla: botany, physiology, and use as a green manure', Economic Botany 34, 111-153. doi: 10.1007/BF02858627

Mahanty T, Bhattacharjee S, Goswami M, Bhattacharyya P, Das B, Ghosh A, Tribedi P. 2017. Biofertilizers: a potential approach for sustainable agriculture development. Environmental Science and Pollution Research 24, 3315-3335. doi: 10.1007/s11356-016-8104-0

Maldonado I, Moreno Terrazas EG, Vilca FZ. 2022. Application of duckweed (Lemna sp.) and water fern (Azolla sp.) in the removal of pharmaceutical residues in water: State of art focus on antibiotics. Science of the Total Environment 838, 1-10. doi: 10.1016/j.scitotenv.2022.156565

Marzouk SH, Tindwa HJ, Amuri NA, Semoka JM. 2023. An overview of underutilized benefits derived from *Azolla* as a promising biofertilizer in lowland rice production. Heliyon 20;9(1):e13040. doi: 10.1016/j.heliyon.2023.e13040.

Meyer C, Lea US, Provan F, Kaiser WM, Lillo C. 2005. Is nitrate reductase a major player in the plant 565 NO (nitric oxide) game? Photosynthesis Research 83, 181–189. https://doi.org/10.1007/s11120-004-3548-3

Mhimdi M, Pérez-Pérez JM. 2020. Understanding of adventitious root formation: what can we learn from comparative genetics?. Frontiers in Plant Science 11, 1–10. doi: 10.3389/fpls.2020.582020

Mongrand S, Hare PD, Chua NH. 2003. Abscisic acid', in Henry, H. and Norman, A. W. (eds) Encyclopedia of Hormones. Riverside (USA): Academic Press. doi: 10.1016/B978-0-12-394807-6.00098-8.

Monteiro MIC, Ferreira FN, de Oliveira NMM, Ávila AK. 2003. Simplified version of the sodium salicylate method for analysis of nitrate in drinking waters. In Analytica Chimica Acta 477(1), 125-129. doi: 10.1016/S0003-2670(02)01395-8

Moore AW. 1969. Azolla: biology and agronomic significance', The Botanical Review 35, 17–34. https://link.springer.com/article/10.1007/BF02859886

Mueller ND, Gerber JS, Johnston M, Ray DK, Ramankutty N, Foley JA. 2012. Closing yield gaps through nutrient and water management. Nature 490(7419), 254-257. doi: 10.1038/nature11420

Muller M. Schmidt W. 2004. Environmentally induced plasticity of root hair development in Arabidopsis. Plant Physiology 134, 409-419. doi: 10.1104/pp

Murashige T, Skoog F. 1962. A revised medium for rapid growth and bio Assays with Tobacco tissue cultures. Plant Physiology 15, 473- 497 doi.org/10.1111/j.1399-3054.1962.tb08052.x

Nguyen NK, Wang J, Liu D, Hwang BK, Jwa NS. 2022. Rice iron storage protein ferritin 2 (OsFER2) positively regulates ferroptotic cell death and defense responses against Magnaporthe oryzae. Frontiers in Plant Science 13, 1-24. doi: 10.3389/fpls.2022.1019669

Nguyen NV. 2002. Global climate changes and rice food security. In FAO. http://www.hechoenperu.org.pe/fao/docs/Agriculture/3-Nguyen.pdf

Pang Z, Chong J, Zhou G, Anderson de Lima Morais DA, Chang L, Barrette M, Gauthier C, Jacques PE, Li S, Xia J. 2021. MetaboAnalyst 5.0: narrowing the gap between raw spectra and functional insights.Nucleic Acids Research 49, 388–396. doi: 10.1093/nar/gkab382.

Peters GA, Meeks JC. 1989. The Azolla-Anabaena Symbiosis: Basic Biology. Annual Review of Plant Physiology and Plant Molecular Biology 40, 193-210. https://doi.org/10.1146/annurev.pp.40.060189.001205

Petit JM, Briat JF, Lobréaux S. 2001. Structure and differential expression of the four members of the Arabidopsis thaliana ferritin gene family. Biochemical Journal 359, 575-582. doi: 10.1042/0264-6021:3590575

Prakash V, Vishwakarma K, Singh VP, Rai P Ramawat N, Tripathi DK, Sharma S. 2020. NO and ROS implications in the organization of root system architecture. Physiologia Plantarum 168, 473–489. doi: 10.1111/ppl.13050.

Prerostova S, Dobrev PI, Knirsch V. 2021. Light Quality and Intensity Modulate Cold Acclimation in Arabidopsis. Int. J. Mol. Sci. 22, 2736. https:// doi.org/10.3390/ijms22052736

Qiao W, Fan LM. 2008. Nitric oxide signalling in plant responses to abiotic stresses. Journal of Integrative Plant Biology 50, 1238-1246. doi: 10.1111/j.1744-7909.2008.00759.x

R Core Team. 2016. R: a language and environment for statistical computing. Vienna, Austria: R Foundation for statistical Computing. https://www.R-project.org/.

Rippka R, Deruelles J, Waterbury JB. 1979. Generic assignments, strain histories and properties of pure cultures of cyanobacteria. Journal of General Microbiology 111, 1-61. doi: 10.1099/00221287

Rivas-San Vicente M, Plasencia J. 2011. Salicylic acid beyond defence: Its role in plant growth and development. Journal of Experimental Botany 62(10) 3321-3338. doi: 10.1093/jxb/err031

Růzicka K, Ljung K, Vanneste S, Podhorská R, Beeckman T, Friml J, Benková E. 2007. Ethylene regulates root growth through effects on auxin biosynthesis and transport- dependent auxin distribution. Plant Cell 19, 2197-2212. doi: 10.1105/tpc.107.052126

Sahay S, Robledo-Arratia L, Glowacka K, Gupta M. 2021. Root NRT, NiR, AMT, GS, GOGAT and GDH expression levels reveal NO and ABA mediated drought tolerance in Brassica juncea L. Scientific Reports 11(1). doi: 10.1038/s41598-021-86401-0

Sakai H, Lee SS, Tanaka T. 2013. Rice annotation project database (RAP-DB): An integrative and interactive database for rice genomics. Plant and Cell Physiology 54, 1–11. doi: 10.1093/pcp/pcs183

Sánchez-Vicente I, Fernández-Espinosa MG, Lorenzo O. 2019. Nitric oxide molecular targets: Reprogramming plant development upon stress. Journal of Experimental Botany 70, 4441-4460. doi: 10.1093/jxb/erz339

Séguéla M, Briat JF, Vert G, Curie C. 2008. Cytokinins negatively regulate the root iron uptake machinery in Arabidopsis through a growth-dependent pathway. Plant Journal 55, 289-300. doi: 10.1111/j.1365- 313X.2008.03502.x

Shannon P, Markiel A, Ozier O, Baliga NS, Wang JT, Ramage D, Amin N, Schwikowski B, Ideker T. 2003. Cytoscape: a software environment for integrated models. Genome Research 13, 2498-2504. doi: 10.1101/gr.1239303.metabolite

Shi DJ, Hall DO. 1988. The Azolla-Anabaena association: historical perspective, symbiosis and energy metabolism. The Botanical Review 54, 353-386. doi: 10.1007/BF02858416

Singh S. 2014. A review on possible elicitor molecules of cyanobacteria: Their role in improving plant growth and providing tolerance against biotic or abiotic stress. Journal of Applied Microbiology 117, 1221-1244. doi: 10.1111/jam.12612

Soneson C, Love MI, Robinson MD. 2015. Differential analyses for RNA-seq: transcript-level estimates improve gene-level inferences. F1000Research 4, 1-19. doi: 10.12688/f1000research.7563.1

Sprangers K, Thys S, van Dusschoten D, Beemster Gerrit TS. 2020. Gibberellin enhances the anisotropy of cell expansion in the growth zone of the maize leaf. Frontiers in Plant Science 11, 1-13. doi: 10.3389/fpls.2020.01163

Stein RJ, Ricachenevsky FK, Fett JP. 2009. Differential regulation of the two rice ferritin genes (OsFER1 and OsFER2). Plant Science 177, 563–569. doi: 10.1016/j.plantsci.2009.08.001

Sun C, Liu L, Yu Y, Liu W, Liu Li, Jin C, Lin X. 2015. Nitric oxide alleviates aluminum-induced oxidative damage through regulating the ascorbate-glutathione cycle in roots of wheat. Journal of Integrative Plant Biology, 57, pp. 550–561. doi:10.1111/jipb.12298.

Tewari RK, Horemans N, Watanabe M. 2021. Evidence for a role of nitric oxide in iron homeostasis in plants. Journal of Experimental Botany 72, 990-1006. doi: 10.1093/jxb/eraa484

Tilman D, Balzer C, Hill J, Befort BL. 2011. Global food demand and the sustainable intensification of agriculture. Proceedings of the National Academy of Sciences of the United States of America 108, 20260-20264. doi:10.1073/pnas.1116437108

Tucuch-Haas CJ, Pérez-Balam JV, Díaz-Magaña KB, Castillo-Chuc JM, Dzib-Ek MG, Alcántar-González G, Vergara-Yoisura S, Larqué-Saavedra A. 2017. N. (eds) Salicylic Acid: A Multifaceted Hormone. Springer, Singapore. doi: 10.1007/978-981-10-6068-7_1

Tung HF, Shen TC. 1985. Studies on Azolla pinnata-Anabaena azollae symbiosis: concurrent growth of Azolla with rice. Aquatic Botany 22,145-152.

United Nations (UN). 2022. 'World Population Prospects 2022. Summary of Results', twenty seventh, New York (USA). www.un.org/development/ desa/pd/.

US EPA. 2007. 'Method 3015A (SW-846): Microwave assisted acid digestion of aqueous samples and extracts', Washington DC (USA). https://www.epa.gov/esam/epa-method-3015a-microwave-assisted-acid-digestion-aqueous-samples-and-extracts

Valette M, Rey M, Doré J, Gerin F, Wisniewski-Dyé F. 2020. Identification of a small set of genes commonly regulated in rice roots in response to beneficial rhizobacteria. Physiology and Molecular Biology of Plants 26, 2537-2551. doi: 10.1007/s12298-020-00911-1

Vishwakarma A, Wany A, Pandey S, Bulle M, Kumari A, Kishorekumar R, Igamberdiev AU, Mur LAJ, Gupta KJ. 2019. Current approaches to measure nitric oxide in plants', Journal of Experimental Botany 70, 4333-4343. doi: 10.1093/jxb/erz242

Vlek PLG, Eberhardt U, Aung MM. 2002. The role of Azolla in lowering the pH of simulated floodwater. Journal of Applied Botany-Angewandte Botanik 76, 1-7. doi: 10.5555/20023068402

Wagner GM. 1997. Azolla: a review of its biology and utilization. The Botanical Review 63, 1–26. The New York Botanical Garden

Watanabe I. 1982. Azolla-Anabaena symbiosis - its physiology and use in tropical agriculture', in Dommergues, Y. R. and Diem, H. G. (eds) Microbiology of Tropical Soils and Plant Productivity. Dordrecht, Netherlands: Springer, pp. 169–185. doi: https://doi.org/10.1007/978-94-009-7529-3_6.

Watanabe I, Liu CC. 1992. Improving nitrogen-fixing systems and integrating them into sustainable rice farming. Plant and Soil 141, 57-67. doi: 10.1007/BF00011310

Wu W, Du K, Kang X, Wei H. 2021. The diverse roles of cytokinins in regulating leaf development. Horticulture Research 8. doi: 10.1038/s41438-021-00558-3

Xiong J, Tao L, Zhu C. 2009. Does nitric oxide play a pivotal role downstream of auxin in promoting crown root primordia initiation in monocots?. Plant Signaling and Behavior 4(10), 999-1001. doi: 10.4161/psb.4.10.9715

Yamasaki H. 2005. The NO world for plants: achieving balance in an open system. Plant, Cell and Environment 28, 78-84. doi: 10.1111/j.1365-3040.2005.01297.x

Yamasaki H, Sakihama Y, Takahashi S. 1999. An alternative pathway for nitric oxide production in plants: new features of an old enzyme. Trends in Plant Science 4, 128-129. doi: 10.1016/S1360-1385(99)01393-X

Yao Y, Zhang M, Tian Y, Zhao M, Zeng K, Zhang B, Zhao M, Yin B. 2018. Azolla biofertilizer for improving low nitrogen use efficiency in an intensive rice cropping system', Field Crops Research, 216, pp. 158–164. doi: 10.1016/j.fcr.2017.11.020.

Yang G, Ji H, Liu H, Feng Y, Zhang Y, Chen L, Guo Z. 2018. Azolla biofertilizer for improving low nitrogen use efficiency in an intensive rice cropping system. Field Crops Research 216, 158-164. doi: 10.1016/j.fcr.2017.11.020

Yu M, Lamattina L, Spoel S H, Loake GJ. 2014. Nitric oxide function in plant biology: A redox cue in deconvolution. In New Phytologist 202(4), 1142–1156. Blackwell Publishing Ltd. https://doi.org/10.1111/nph.12739

Yuan HM, Liu WC, Jin Y, Lu YT. 2013. Role of ROS and auxin in plant response to metal-mediated stress. Plant Signalling and Behavior 8(7): e24671. doi: 10.4161/psb.24671

Zahir ZA, Asghar HN, Arshad M. 2001. Cytokinin and its precursors for improving growth and yield of rice. Soil Biology & Biochemistry 33, 405-408.

Zhang X, Xue C, Wang R, Shen R, Lan P. 2022. Physiological and proteomic dissection of the rice roots in response to iron deficiency and excess. Journal of Proteomics 267, 1-15.

Zhao B, Liu Q, Wang B, Yuan F. 2021. Roles of Phytohormones and Their Signaling Pathways in Leaf Development and Stress Responses. Journal of Agricultural and Food Chemistry 69(12), 3566-3584. doi: 10.1021/acs.jafc.0c07908

Zhao DY, Tian QY, Li LH, Zhang WH. 2007. Nitric oxide is involved in nitrate-induced inhibition of root elongation in Zea mays. Annals of Botany 100, 497-503. doi: 10.1093/aob/mcm142

Zhao J, Yu N, Ju M, Fan B, Zhang Y, Zhu E, Zhang M, Zhang K. 2019. ABC transporter OsABCG18 controls the shootward transport of cytokinins and grain yield in rice. Journal of Experimental Botany 70, 6277-6291. doi: 10.1093/jxb/erz382

Zhao Y, Zhang W, Abou-Elwafa SF, Shabala S, Xu L. 2021. Understanding a mechanistic basis of ABA involvement in plant adaptation to soil flooding: The current standing. Plants 10, 1-15. doi: 10.3390/plants10101982

Zhou B, Guo Z, Xing J, Huang B. 2005. Nitric oxide is involved in abscisic acid-induced antioxidant activities in Stylosanthes guianensis. Journal of Experimental Botany 56, 3223-3228. doi: 10.1093/jxb/eri319

Table 1. NO-related DEGs at 15 DAT

RAP-DB	Symbol	Log2FC	padj	Description
Os02g0770800	*NR2/NIA1/NIA2*	5.373	8.4E-05	*NADH/NADPH-dependent nitrate reductase*
Os10g0554200	*NRT1.1B/NPF6.5*	3.049	3.9E-04	*Nitrate transporter 1.1B*
Os10g0169900	*NRT*	4.308	1.6E-04	*Nitrate and chloride transporter*

Figure legends

Figure 1 - Effect of *A. filiculoides* on the number (A) and length (B) of ARs in rice at 15, 30 and 60 DAT, and on the number of LRs of rice at 15 (C) and 30 DAT (D). Bar Graphs represent mean values ± SE of control rice (R) and rice grown with A. filiculoides (R+Af). A: 15 DAT R n = 6; 15 DAT R + Af n = 7; 30 DAT R and R+Af n = 18; 60 DAT R n = 7; 60 DAT R + Af n = 9. B: 15 DAT R n = 144; 15 DAT R + Af n = 187; 30 DAT R n = 254; 30 DAT R + Af n = 333; 60 DAT R n = 853; 60 DAT R + Af n = 1711. C and D: 15 and 30 DAT, respectively. R n = 10; R + Af n = 11. ***, P < 0.001.
*, P < 0.05.

Figure 2 - Effect of *A. filiculoides* on the relative amount of NO in the ARs of rice at 15 and 30 DAT. Bar Graphs represent mean values ± SE of control rice (R) and rice grown with A. filiculoides (R + Af). 15 DAT R n = 23; 15 DAT R+Af n = 22; 30 DAT R and R + Af n = 15; 60 DAT R n = 21. ***, P < 0.001. CTCF: Corrected Total Cell Fluorescence. Pictures were taken at the fluorescence microscope, and picture analysis was performed in ImageJ. Data shown do not take into account sample autofluorescence.

Figure 3 - Effect of *A. filiculoide*s on the number of leaves (A), plant height (B), number of tillers (C) and root/shoot fresh weights (D) over two months. Linear Graphs represent mean values ± SE of control rice (R) and rice grown with *A. filiculoides* (R+Af). Linear graphs: 0, 7, 15, 20, 28 DAT R and R+Af n= 12; 34 and 39 DAT R n= 11; 34 and 39 DAT R + Af n = 12; 46, 53 and 60 DAT R n= 8; 46, 53 and 60 DAT R+Af n=9. Bar graphs: 15 DAT R n=6; 15 DAT R + Af n=7; 30 DAT R and R + Af n=20; 60 DAT R n=12; 60 DAT R + Af n=15 *, P < 0.05; **, P < 0.01; ***, P < 0.001.

Figure 4 - PCA (A) and DE gene count at 15 DAT (B).

Figure 5 - The 20 most enriched BP (A) and MF (B) terms among the DEGs in rice roots at 15 DAT.

Figure 6 – Schematic representation of the iron acquisition systems in rice roots. Under Strategy I the ferric chelate complex is reduced to ferrous ion by FRO. H^+ released by the proton pump acidifies the medium to convert ferric ion to ferrous ion. IRTs transport the ferrous ion into the root cells. VITs are responsible for transportation and accumulation of iron within the vacuole while FERs are the proteins accommodating excess iron within the cells. Under Strategy II, MA phytosiderophores, produced by the sequential activity of NAS, NAAT and DMA, chelate Fe(III). Chelated Fe(III) complex is transported across the membrane into the root cell by YSLs. Green and red arrows refer to transporters/enzymes whose mRNA are increased and decreased, respectively, in the R+Af vs R treatment. For the differential expression of regulatory genes refer to TableS4. The picture was redrawn from Kar and Panda (2020) and Kobayashi *et al.*, (2014).

Figure 7 - Network analysis of DEGs. The functional categories are linked if they shared ≥ 20% genes (FDR cut-off = 0.05).

Figure 8 - Genes expression profiles of selected DEGs at 15 DAT as resulted from the qRT-PCR analysis at 0, 5, 9 12 and 15 DAT. Asterisks indicate significant differences between the two treatments at a given time pint (t-test, $P < 0.05$), while letters indicate significant differences between time points of the same treatment (ANOVA, $P < 0.05$; Tukey's HSD, $P < 0.05$).

Figure 9 - Differential levels of hormonal compounds in the roots of rice grown with and without *A. filiculoides* at 15 DAT. Unpaired two samples t-test for all five compounds except IAA-Glu, for which the unpaired two samples Wilcoxon test was performed. For all five compounds: $P < 0.01$, FDR cut-off ≤ 0.05. See also Table S8.

Figure 10 - Accumulation profiles at 0 and 15 DAT of the bioactive hormones in rice roots (A) and leaves (B) from R+Af and R treatments.

Supplementary data

Table S1 - DEGs and housekeeping genes investigated by qRT-PCR analysis.

Table S2 - Levels of inorganic nitrogen forms in growth media at 10, 20 and 30 DAT.

Table S3 - DEGs of the methionine savage pahway (MPS).

Table S4 - DEGs involved in iron absorption and homeostasis.

Table S5 - DEGs related to ROS scavenging/homeostasis.

Table S6 - DEGs involved in hormone processing and signalling.

Table S7 - Compounds investigated by targeted-hormonomics.

Table S8 - Detected and quantified hormonal compounds in the roots of rice grown in the R+Af compared to the R treatment at 15 DAT.

Table S9 - Detected and quantified hormonal compounds in the roots of rice grown in the R and R+ Af treatments over time, 0 and 15 DAT.

Table S10 - Detected and quantified hormonal compounds in the leaves of rice grown in the R+Af compared to the R treatment at 15 DAT.

Table S11 - Detected and quantified hormonal compounds in the leaves of rice grown in the R and R+Af treatments over time, 0 and 15 DAT.

Table S12 - Detected and quantified hormonal compounds in the media of rice grown in the R+Af compared to the R treatment at 15 DAT.

Figure S1 - Effect of *A. filiculoides* on the biomass of the root apparatus of rice at 15, 30 and 60 DAT. Bar Graphs represent mean values ± SE of control rice (R) and rice grown with *A. filiculoides* (R + Af). $P > 0.05$.

Figure S2 - Effect of *A. filiculoides* on the relative amount of NO in the ARs of rice at 15 and 30 DAT quantified via Griess assay. Bar Graphs represent mean values ± SE of control rice (R) and rice grown with *A. filiculoides* (R+Af) treatments. *, $p < 0.05$.

Figure S3 - Effect of *A. filiculoides* on the above ground part and total biomass of rice (also refer to Fig. 12) at 15, 30 and 60 DAT. Bar Graphs represent mean values ± SE of control rice (R) and rice grown with *A. filiculoides* (R+Af). *, $P < 0.05$; **, $P < 0.01$.

Figure S3 - Plots of the fold enrichment of the upregulated DEGs. A: BP and B: MF. BP: biological process; MF: molecular function.

Figure S5 - Plots of the fold enrichment of the downregulated DEGs. A: BP and B: MF. BP: biological process; MF: molecular function.

Figure S6 - sPLSDA (A) and sPLSDA corresponding loadings plot (B) of the most discriminant phytohormones explaining replicates' distribution in the roots of rice grown with (R+Af) and without *A. filiculoides* (R) at 15 DAT. The higher the Loadings value on the x-axis, the more discriminant the compound (B).

Figure S7 - sPLSDA (A) and sPLSDA corresponding loadings plot (B) of the most discriminant compounds explaining replicates classification in the leaves of rice grown in the R+Af and R treatments at 15 DAT.

Figure S8 - Significantly different levels of hormonal compounds in the leaves of rice grown with and without *A. filiculoides* at 15 DAT. Unpaired two samples t-test for all nineteen compounds; $P < 0.01$; FDR cut-off ≤ 0.001. See also Table S12.

Figure S9 - sPLSDA (A) and corresponding loadings plot (B) of the most discriminant phytohormones explaining treatments' variance in the media in the R+Af and R treatments at 15 DAT.

Figure S10 – Significant different levels of hormonal compounds in the R+Af and R media at 15 DAT. Unpaired two samples t-test for all four compounds; $P < 0.05$. See also Table S11.

Figure S11 - Differential levels of hormonal compounds in the control and *T. azollae*-growing (Ta) media after 7 days of growth.

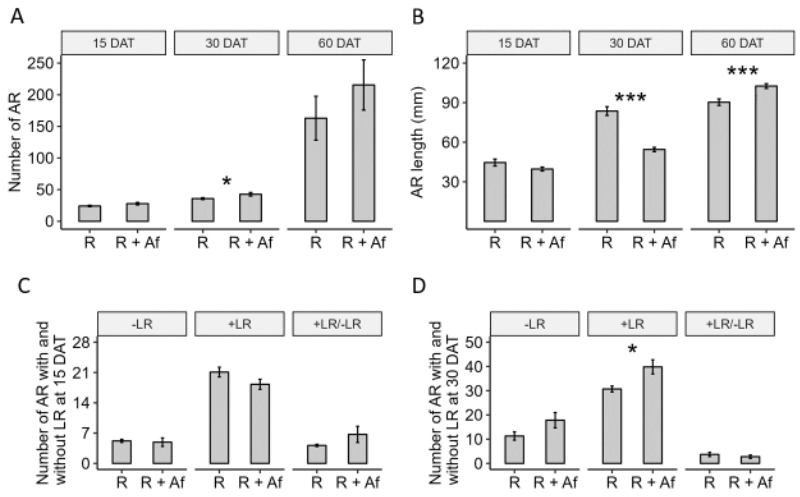
A
15 DAT
30 DAT
60 DAT
Number of AR
250
200
150
100
50
0
*
R
R + Af
B
AR length (mm)
120
90
60
30
***
***
C
-LR
+LR
+LR/-LR
Number of AR with and without LR at 15 DAT
28
21
14
7
0
D
Number of AR with and without LR at 30 DAT
50
40
30
20
10
0
*

Figure 1

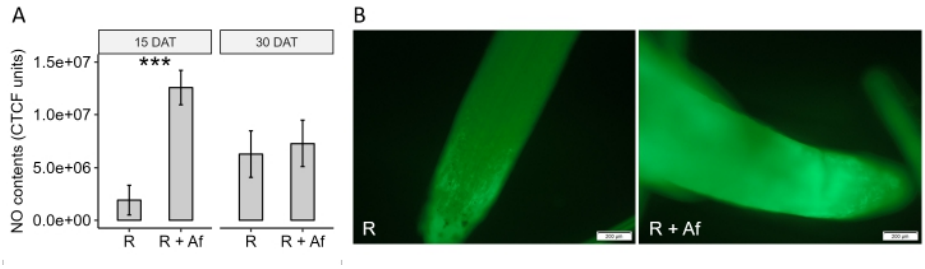
A
15 DAT
30 DAT
***
NO contents (CTCF units)
1.5e+07
1.0e+07
5.0e+06
0.0e+00
R
R + Af
R
R + Af
B
R
R + Af

Figure 2

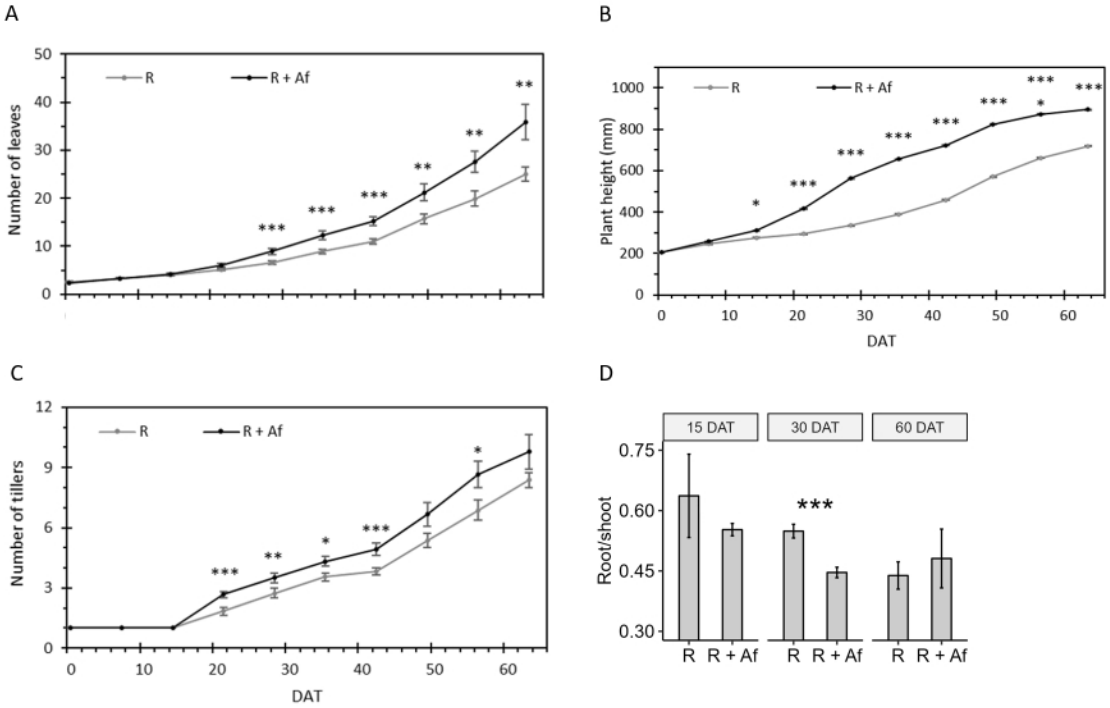
A
B
C
D
R
R + Af
Number of leaves
Plant height (mm)
Number of tillers
DAT
Root/shoot
15 DAT
30 DAT
60 DAT

Figure 3

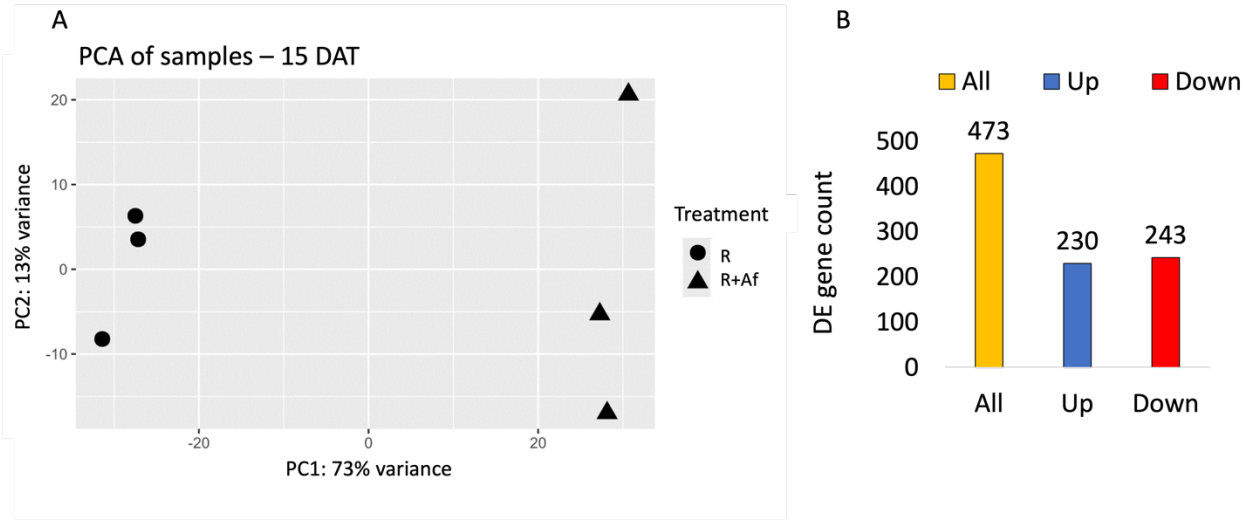
A
PCA of samples – 15 DAT
PC2: 13% variance
PC1: 73% variance
20
10
0
-10
-20
0
20
Treatment
R
R+Af
B
All
Up
Down
DE gene count
500
400
300
200
100
0
473
230
243
All
Up
Down

Figure 4

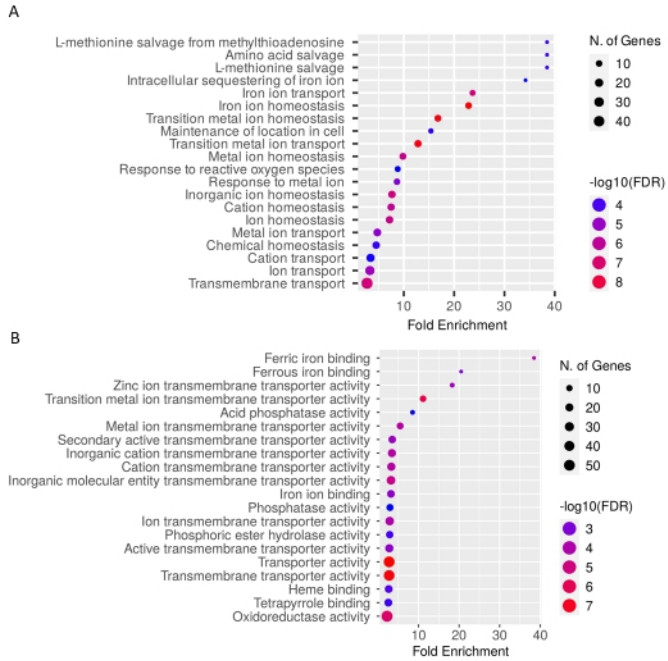
A
L-methionine salvage from methylthioadenosine
Amino acid salvage
L-methionine salvage
Intracellular sequestering of iron ion
Iron ion transport
Iron ion homeostasis
Transition metal ion homeostasis
Maintenance of location in cell
Transition metal ion transport
Metal ion homeostasis
Response to reactive oxygen species
Response to metal ion
Inorganic ion homeostasis
Cation homeostasis
Ion homeostasis
Metal ion transport
Chemical homeostasis
Cation transport
Ion transport
Transmembrane transport
10
20
30
40
Fold Enrichment
N. of Genes
10
20
30
40
-log10(FDR)
4
5
6
7
8
B
Ferric iron binding
Ferrous iron binding
Zinc ion transmembrane transporter activity
Transition metal ion transmembrane transporter activity
Acid phosphatase activity
Metal ion transmembrane transporter activity
Secondary active transmembrane transporter activity
Inorganic cation transmembrane transporter activity
Cation transmembrane transporter activity
Inorganic molecular entity transmembrane transporter activity
Iron ion binding
Phosphatase activity
Ion transmembrane transporter activity
Phosphoric ester hydrolase activity
Active transmembrane transporter activity
Transporter activity
Transmembrane transporter activity
Heme binding
Tetrapyrrole binding
Oxidoreductase activity
10
20
30
40
Fold Enrichment
N. of Genes
10
20
30
40
50
-log10(FDR)
3
4
5
6
7

Figure 5

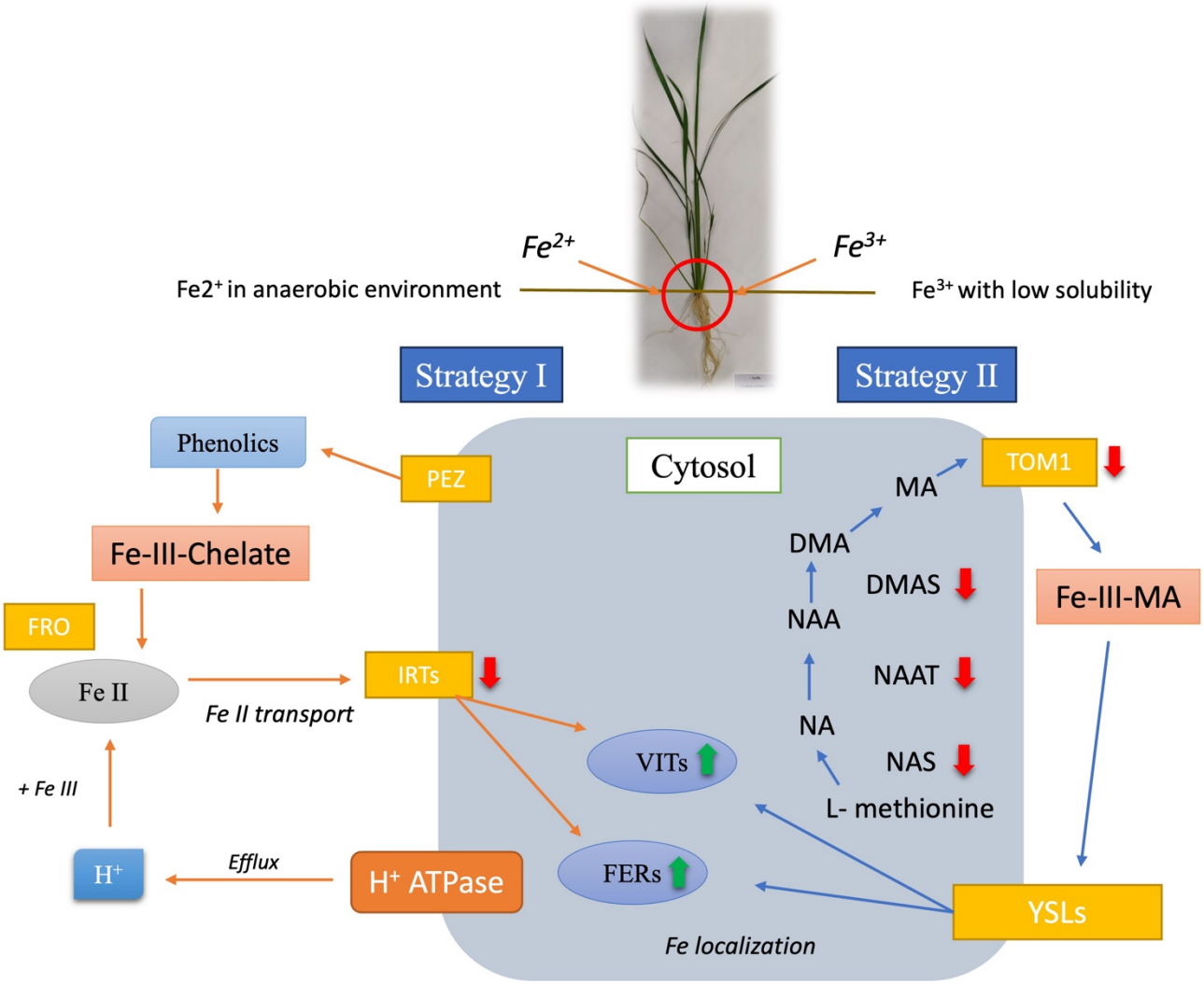
Fe2+ in anaerobic environment
Fe2+
Fe3+
Fe3+ with low solubility
Strategy I
Strategy II
Phenolics
PEZ
Cytosol
TOM1
MA
DMA
DMAS
NAA
NAAT
NA
NAS
L- methionine
Fe-III-Chelate
Fe-III-MA
FRO
Fe II
IRTs
Fe II transport
VITs
+ Fe III
H+
Efflux
H+ ATPase
FERs
YSLs
Fe localization

Figure 6

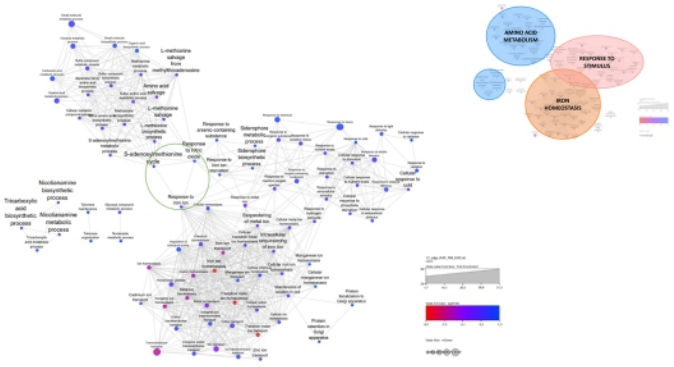
AMINO ACID METABOLISM
RESPONSE TO STIMULUS
IRON HOMEOSTASIS

Figure 7

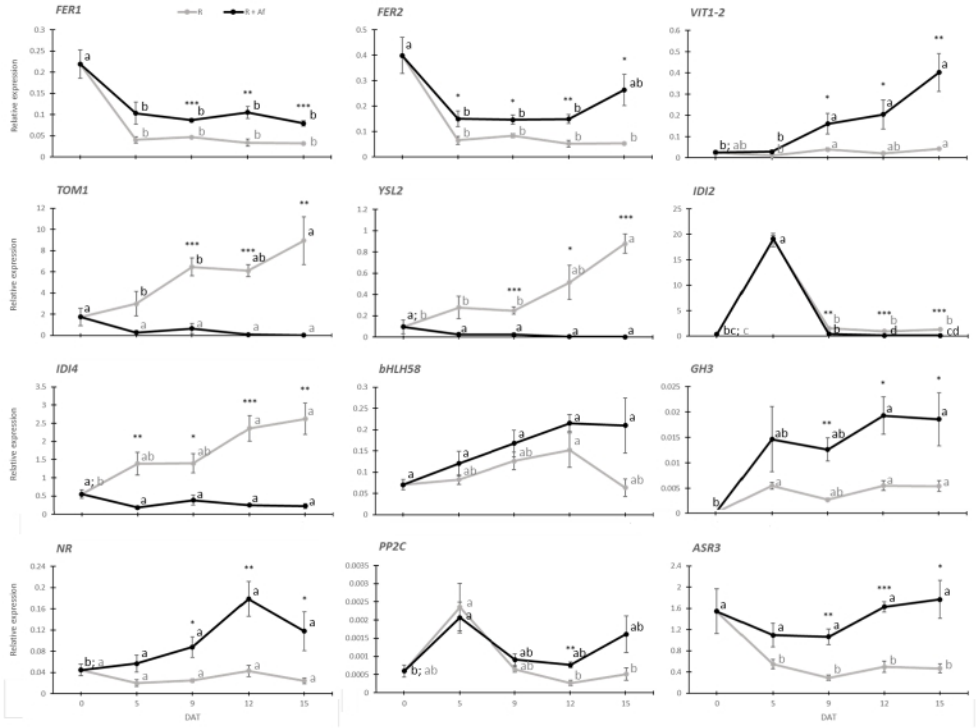
FER1
R
R + Af
FER2
VIT1-2
TOM1
YSL2
IDI2
IDI4
bHLH58
GH3
NR
PP2C
ASR3
Relative expression
DAT

Figure 8

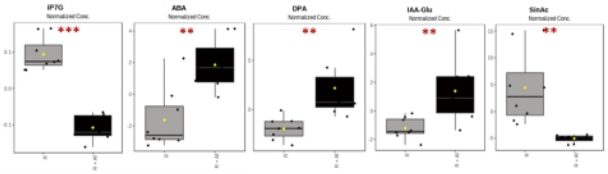
IP7G
Normalized Conc.
ABA
Normalized Conc.
DPA
Normalized Conc.
IAA-Glu
Normalized Conc.
SinAc
Normalized Conc.

Figure 9

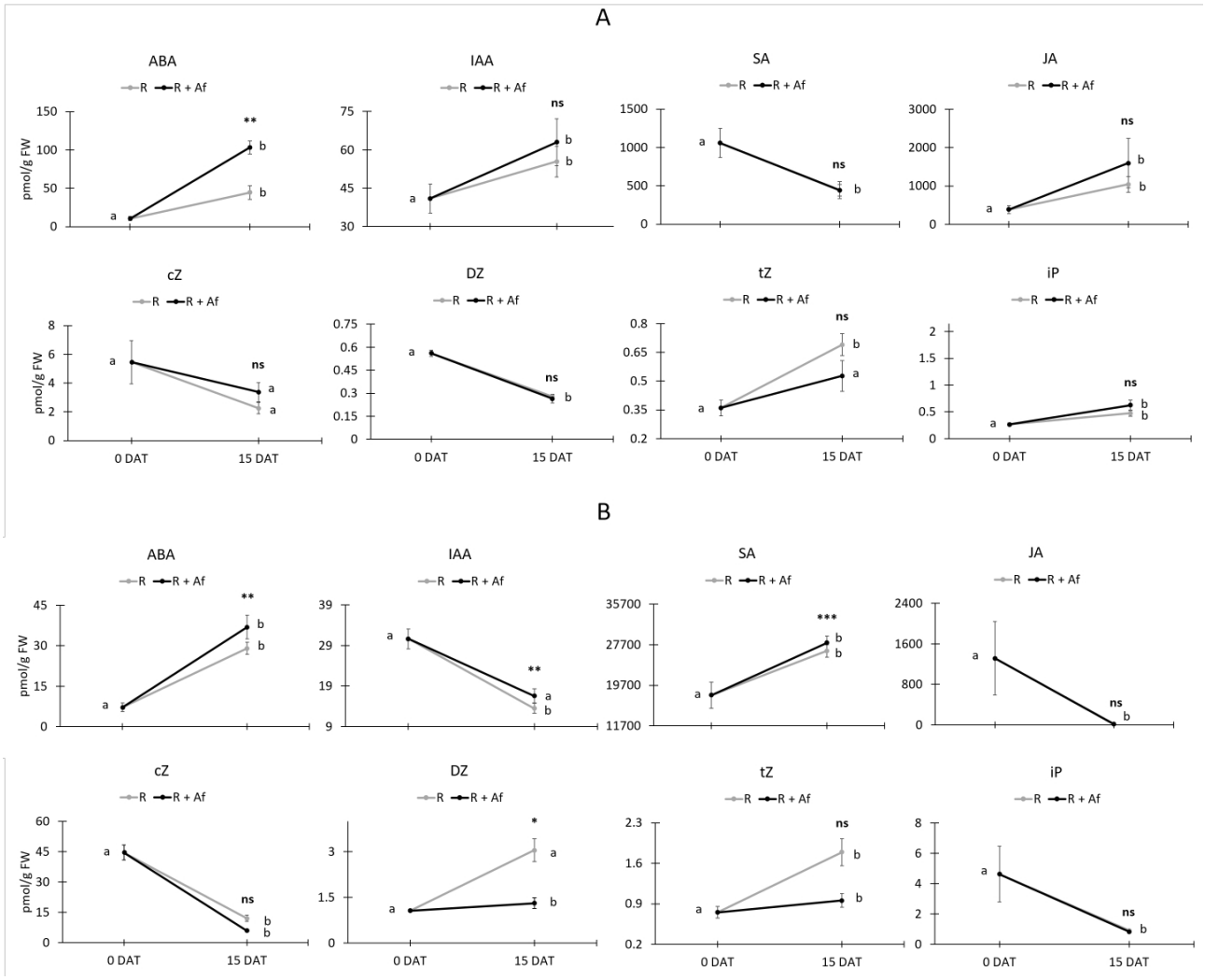

Figure 10